Original article

Ukrainian Neurosurgical Journal. 2026;32(1):69-91
doi: 10.25305/unj.341693

Development and validation of a multilevel scale for quantitative assessment of mechanical exposure in traumatic spinal injuries

Oleksii S. Nekhlopochyn [1], Vadim V. Verbov [2], Ievgen V. Cheshuk [2], Milan V. Vorodi [2]

[1] Spine Surgery Department, Romodanov Neurosurgery Institute, Kyiv, Ukraine
[2] Restorative Neurosurgery Department, Romodanov Neurosurgery Institute, Kyiv, Ukraine

Received: 19 October 2025
Accepted: 14 November 2025

Address for correspondence:
Oleksii S. Nekhlopochyn, Spine Surgery Department, Romodanov Neurosurgery Institute, 32 Platona Maiborody st., Kyiv, 04050, Ukraine, e-mail: AlexeyNS@gmail.com

Objective: To develop, theoretically substantiate, and perform primary validation of a multilevel (0–10 points) scale for quantitative assessment of the intensity of external mechanical impact in traumatic spinal injuries.

Materials and methods: The study design followed the COSMIN (Consensus-based Standards for the Selection of Health Measurement Instruments) principles for developing and validating medical measurement tools, ensuring an adequate level of scientific validity and reproducibility. A literature review (PubMed, Scopus, Web of Science, 1990–2025) enabled the identification of threshold values and modifying factors, including patient body mass, the transmission coefficient of impulse ($T_{land)}$), and the effective deceleration distance (S_{land}). Two datasets were used for validation: 40 standardized clinical vignettes and 52 real cases of thoracolumbar junction trauma (T11–L2) with mandatory verification by computed tomography/magnetic resonance imaging. Construct and criterion validity, inter-rater reliability (ICC, κ), absolute reliability (SEM, MDC_{95}), diagnostic accuracy (ROC analysis), agreement level (Bland–Altman), and threshold stability were assessed.

Results: Based on comparative analysis of various approaches, the concept of "equivalent fall height" was proposed as a universal criterion of mechanical exposure in spinal trauma. An 11-level (0–10) quantitative scale and a spine-oriented derived metric were developed. Primary validation demonstrated high inter-rater agreement (ICC(2,1): 0.84 for the basic indicator and 0.79 for the spinal-oriented one; ICC(2,k): 0.95 and 0.92), acceptable absolute precision (SEM 0.80–0.95; MDC_{95} 2.2–2.6 points), and stable thresholds (discrepancies exceeding ±1 level occurred in <7% of cases). The metrics showed significant associations with vertebral body wedge deformity (r=0.58), spinal canal compromise (r=0.49), and ordinal injury severity by AO Spine (ρ=0.62; p<0.001). In logistic modeling, each additional 1 m in equivalent fall height nearly doubled the odds of burst/unstable injuries (OR=1.85; 95% CI 1.45–2.38). The diagnostic performance of the scale was confirmed (AUC=0.82) for identifying vertebral fractures (optimal threshold ≈1.3 m; sensitivity – 0.76; specificity – 0.72).

Conclusions: The proposed scale provides a quantitative, mass-neutral, and clinically interpretable measure of the "event severity," complements morphological classifications, enhances risk stratification, and can be applied for patient triage, diagnostic planning, and multicenter research.

Keywords: *spinal trauma; thoracolumbar junction; mechanical exposure; equivalent fall height; spinal-equivalent height; quantitative scale; measurement instrument validation; individualization.*

Introduction

Traumatic injuries of the spine constitute a heterogeneous group of conditions resulting from exposure to a wide spectrum of mechanical factors, ranging from low-energy events (e.g., falls from standing height) to high-energy mechanisms (falls from significant height, road traffic accidents (RTAs), sports-related and blast injuries) [1, 2]. According to population-based studies, the annual incidence of spinal trauma is 23–40 cases per 100,000 population, of which 15–20% are accompanied by neurological deficits of varying severity [2]. These estimates, however, require careful interpretation in light of methodological differences across studies and geographic regions.

Spinal injuries may arise from either direct or indirect mechanisms. Direct injury develops following the immediate application of force to the vertebral column (impact by a heavy object, gunshot or stab wounds, compression between massive objects) [3]. Such injuries are relatively uncommon and more

frequently limited to localized damage of the spinous and transverse processes or adjacent soft tissues. In contrast, the indirect mechanism—responsible for more than 90% of spinal injuries in peacetime—results from the transmission of external force to the body as a whole [1, 4]. This category includes falls of various types and RTAs, in which spinal damage occurs due to axial loading, flexion–rotation, or combined forces [3, 5–8].

In international clinical practice, fractures occurring under low-energy impact—defined as mechanical force that would not normally compromise bone integrity—are traditionally classified as fragility fractures (osteoporotic fractures) [9]. A classic example is a fall "from standing height or less" [10, 11]. This definition is reflected in World Health Organization (WHO) documents and is widely adopted in contemporary clinical guidelines [9, 12]. At the opposite end of the energy spectrum are high-energy mechanisms: in U.S. prehospital protocols, a fall in an adult from a height exceeding 20 feet (~6 m) has historically been regarded as a marker of high kinetic energy and increased risk of polytrauma [13]. More recent materials from the American College of Surgeons reference a lower threshold (>10 feet), underscoring the variability of cutoff values and the need for terminological standardization [14, 15].

Most widely used classification systems in vertebrology and traumatology focus on the characteristics of the injury outcome rather than on quantitative assessment of the intensity of external exposure [16]. For instance, the Abbreviated Injury Scale (AIS) is an anatomically based six-point system for grading injury severity by body region [17, 18], whereas the AO Spine Thoracolumbar Classification system categorizes thoracolumbar injuries according to morphological type (A, B, C), neurological status, and modifiers (including assessment of the integrity of the posterior ligamentous complex) [19–21]. These tools are indispensable for standardized injury description, risk stratification, and treatment planning; however, they do not provide a quantitative characterization of the "energy of the event" (mechanical exposure) preceding injury development [16].

In routine clinical practice, the mechanism of trauma is often described in simplified binary or qualitative terms ("low-/high-energy injury," "mild/severe"), which fail to reflect the continuous nature of mechanical exposure gradients and may lead to the loss of clinically relevant information [22, 23]. The absence of a standardized quantitative instrument complicates cohort comparisons and interpretation of research findings, and limits the potential for targeted preventive and rehabilitative strategies [24]. In this context, the development of a multilevel scale for the quantitative assessment of external mechanical impact intensity is warranted. Such a scale should be grounded in fundamental principles of mechanics (energy, impulse, acceleration) and be applicable in real-world clinical settings. A key methodological step is the introduction of a universal metric that enables different injury mechanisms to be translated into a unified energy scale, thereby standardizing the description of the "force of the event" for clinical communication and scientific analysis [5, 25].

Objective: To develop, theoretically substantiate, and conduct primary validation of a multilevel (0–10 points) scale for the quantitative assessment of the intensity of external mechanical impact in traumatic spinal injuries.

Materials and methods

The study design conforms to the principles of COSMIN (Consensus-based Standards for the Selection of Health Measurement Instruments) for the development and validation of measurement instruments in medicine, thereby ensuring an adequate level of scientific rigor and reproducibility of the obtained results [26, 27].

The literature search was conducted in two stages**.**

Stage 1 (analytical review of scales and terminology). The objective was to identify classification systems/scales, threshold values, and underlying principles used in clinical practice and guidelines that are necessary for formulating the conceptual framework of the proposed scale. Keywords: *AO Spine thoracolumbar classification, TLICS, Abbreviated Injury Scale, Injury Severity Score, spinal injury classification reliability, CDC field triage guidelines, mechanism of injury, fall height threshold, fall >10 ft, standing height or less, fragility fracture, osteoporotic vertebral fracture, mechanical exposure, energy of event, biomechanics of spinal injury.*

Stage 2 (collection of quantitative reference parameters). The objective was to determine threshold benchmarks for grading falls and to establish typical ranges/median values of parameters used in constructing the scale (collision scenarios, impulse transmission to the spine, effective stopping distance, environmental/surface modification factors). Keywords: *delta-v estimation, rollover, mass ratio, coefficient of restitution, impact angle, EDR, spine load transmission, landing biomechanics, knee flexion, energy absorption, feet-first, buttocks impact, supine impact, seat belt, airbag, torso kinematics, effective stopping distance, impact attenuation, concrete, asphalt, sand, snow, water entry, gym mat, tatami, HIC, g-max, fall from height, injury severity threshold adults, fragility fracture standing height.*

Databases and search parameters: PubMed/MEDLINE, Scopus, Web of Science; materials from AO Spine, the World Health Organization, and the International Osteoporosis Foundation. Language of publication: English; time frame: 1990–2025 (with no strict lower limit for fundamental biomechanical studies).

Screening was performed in stages by two independent reviewers (initially by titles and abstracts, followed by full-text assessment), with additional searches conducted through the reference lists of selected articles.

Datasets

Validation was performed using two complementary datasets:

Standardized clinical scenarios (vignettes) (n = 40) — synthetic clinical–biomechanical events uniformly covering the spectrum of mechanical exposure (including "adjacent" combinations of body position/surface/deceleration pathway), developed for independent expert assessment according to a standardized protocol.

This article contains some figures that are displayed in color online but in black and white in the print edition.

Real clinical cases (n = 52) — medical records of patients with sufficiently detailed descriptions of the injury mechanism, which, in the authors' judgment, allowed unambiguous reconstruction of the initial parameters required for calculations. In all cases, neuroimaging data (computed tomography (CT) and/or magnetic resonance imaging (MRI)) were available, enabling comparison of mechanical exposure values with morphological injury characteristics, determination of injury type according to the AO Spine classification, assessment of the degree of anterior wedge deformity, extent of spinal canal compromise, and integrity of the posterior ligamentous complex. Image analysis and measurements were performed using RadiAnt DICOM Viewer (Medixant, Poland; version 2023.1, license No. 1860F047).

For primary validation and reduction of interindividual variability, the sample included patients with injuries of the thoracolumbar junction (T11–L2).

Informed consent was obtained from all patients for data collection, processing, and publication of aggregated results in compliance with confidentiality standards. The data provided to experts were fully anonymized.

Sample size determination

To assess inter-rater reliability (intraclass correlation coefficient, ICC) in a design involving five experts, the study aimed to demonstrate an ICC of approximately 0.80 compared with a threshold value of 0.60, at α = 0.05 and statistical power of 0.80. The required sample size was estimated at 35–40 objects [28]. Accordingly, a set of 40 standardized vignettes was constructed, yielding 200 independent ratings (5 × 40), enabling test–retest assessment on a subsample of 10 vignettes [29] and improving the precision of the standard error of measurement (SEM) and the minimal detectable change at the 95% confidence level (MDC_{95}) [30, 31]. For clinical validation, 52 consecutive patients with complete datasets (detailed mechanism description plus CT/MRI data) were included. This sample size provides adequate power for key validity analyses (correlation coefficients r ≈ 0.5–0.6; known-groups comparisons with effect size d ≈ 1.1) [32–34] and acceptable precision for agreement analysis using the Bland–Altman method [35–37]. Receiver operating characteristic (ROC) analysis and regression modeling were considered secondary analyses, with correspondingly wider expected confidence intervals (CIs) [38,39].

Statistical analysis

Data were processed using descriptive and analytical statistical methods. Continuous variables are presented as mean ± SD or median [IQR], depending on distribution characteristics (normality assessed visually and using the Shapiro–Wilk test) [40, 41]. Construct and criterion validity were evaluated by correlation analysis with calculation of Pearson's (r) or Spearman's *(ρ)* coefficients, as appropriate [42, 43].

Predictive models. To assess the association between the proposed metrics and morphological injury severity according to the AO Spine classification, binary logistic regression was applied using a threshold of ≥A3, with estimation of odds ratios (ORs) and 95% CIs [44, 45]. As a sensitivity analysis for the ordinal outcome A1–A4, ordinal logistic regression was performed [46, 47]. Linearity of the logit was examined using the Box–Tidwell test [48] and restricted cubic splines [49, 50], while multicollinearity was assessed by the variance inflation factor (VIF) [51]. Discriminative performance was evaluated using ROC curves (AUC, with 95% CI) [52]. Sensitivity, specificity, the Youden index, and likelihood ratios (LR+, LR–) were calculated. Operational thresholds were selected by maximizing the Youden index, taking into account the intended purpose (screening vs. confirmation) [53].

The robustness of scale boundaries was examined through sensitivity analysis by varying threshold parameters by ±10–15% and recalculating results for alternative modifier scenarios [54, 55].

Known-groups validity. Comparisons were conducted for predefined clinically relevant groups [56]. Between-group differences were analyzed using the Mann–Whitney U test, with nonparametric effect sizes calculated as Cliff's δ [57] and/or Vargha–Delaney A [58]. Cohen's *d* was additionally reported (for reference), with robust interpretation in the presence of unequal variances [59].

Measurement reliability. Relative reliability was assessed through inter-rater agreement indices: ICC(2,1) (two-way random-effects model, absolute agreement, single measure) and ICC(2,k) (average measure) [60], as well as weighted κ with quadratic weights [61, 62]. Temporal stability was evaluated using a test–retest design in a subsample of cases [63]. Agreement between expert-based and algorithm-based calculations was assessed using the Bland–Altman method (mean bias and 95% limits of agreement) [64].

Absolute reliability. SEM and the MDC_{95} (MDC_{95} = 1.96 × √2 × SEM) were calculated [65]. For appropriate clinical interpretation, MDC was additionally expressed in continuous units: in meters for and in multiples of *g* for the spine-oriented metric (based on a reference stopping distance s_{ref} = 0.10 m), with level-specific (interval-specific) annotations indicating the ranges in which differences are clinically negligible or clinically meaningful [66].

All tests were two-sided. The threshold for statistical significance was set at $p < 0.05$ [67, 68].

Statistical analysis was performed using R version 4.5.1 (R Core Team) within RStudio IDE 2025.05.1+513 (Posit) [69].

Results

Definition of the criterion

The intensity of external mechanical impact during a traumatic event is defined as a quantitative characteristic of the force of the event preceding tissue damage [70, 71]. It is not identical to the severity of the resulting injury, which is determined using clinical outcome scales (e.g., the Abbreviated Injury Scale (AIS)) or morphological classifications (e.g., the AO Spine Thoracolumbar Classification) [72]. In contrast to AIS/AO classifications, which focus on anatomical and clinical consequences (type of disruption, instability, neurological status), the proposed criterion captures the mechanical exposure itself—that is, the physical quantity reflecting the amount of mechanical energy/impulse involved in the event [25].

As a universal physical metric, the "equivalent fall height" (h_{eq}) was selected [73, 74]. The underlying concept is that heterogeneous mechanisms (falls,

collisions, compression, blast effects) can, with certain assumptions, be translated onto a unified energy scale by equating them to a hypothetical fall from a given height in a uniform gravitational field. This metric is based on gravitational potential energy and enables comparison of events in terms of "energetically equivalent meters."

In selecting an appropriate physical metric (criterion) for assessing the degree of external mechanical impact on the spine, the following considerations were taken into account:

- first, falls from height represent the most common cause of traumatic spinal injuries. According to the Global Burden of Disease study, falls are the leading cause of vertebral trauma, accounting for 52.2% of spinal injuries and 63.0% of spinal cord injuries [75, 76]. Thus, more than half of traumatic events are attributable to falls, making a height-based scale the most relevant framework [77].

- second, the parameter "fall height" offers important practical advantages [13]. This criterion is intuitively understandable not only for specialists but also for patients and their relatives. A statement such as "a fall from the second floor" immediately conveys an impression of impact intensity [15, 78, 79]. Moreover, this parameter is readily obtainable from clinical documentation [80]. During history taking, patients or witnesses almost invariably refer to "a step and a fall" or "from a height of…," whereas quantitative data for RTAs (velocity), interpersonal violence (type of weapon), or compression injuries are often unavailable or difficult to interpret [81].

- third, falls encompass both the lower and upper limits of the mechanical action spectrum (low-energy and high-energy trauma). Consequently, they provide a broad and clinically relevant range of mechanical exposure [77].

- fourth, the approach is grounded in physical principles. The definition of h_{eq} in terms of fall height follows directly from the laws of mechanics (since potential energy $\Delta E = mgh$), thereby preserving maximal objectivity, avoiding subjective weighting coefficients in estimating impact force, and enabling quantitative comparison of diverse injury mechanisms within a unified physical scale [1, 15, 73].

Analysis of contemporary literature demonstrates that, when characterizing the severity of mechanical impact on the spine based on fall height, only two primary threshold benchmarks are effectively employed.

The first threshold is approximately 1 m. A fall from standing height (~1 m) or less is traditionally regarded as a low-energy mechanism, in which fractures indicate pathological bone fragility (osteoporotic fractures) [82, 83]. This definition is incorporated into recommendations of the World Health Organization and the International Osteoporosis Foundation and is widely applied in clinical practice for risk stratification and the initiation of secondary prevention [84–86].

The second threshold is 20 feet (~6 m). A fall in an adult from a height exceeding 20 feet has historically been recognized as a marker of severe mechanical impact in prehospital medical and trauma triage protocols (CDC, American College of Surgeons). This criterion is associated with a high probability of polytrauma and the need for transport to a specialized trauma center [87]. Although some contemporary guidelines discuss a lower universal threshold (>10 feet), 20 feet remains the most frequently cited "upper" benchmark of high-energy trauma.

Thus, in routine practice, only two quantified reference values are used when describing the mechanism of injury: ~1 m as the boundary of low-energy exposure and ~6 m as an indicator of high-energy trauma (***Fig. 1***). The intermediate range remains insufficiently formalized [15, 88, 89].

Intensity of overall external mechanical impact – fall scenario

To enhance the precision of stratifying the mechanical factor in traumatic spinal injuries, an 11-level scale for grading the intensity of external impact was developed based on our clinical experience and analysis of the literature [3, 5, 70, 90]. Unlike binary or simplified classifications, the proposed system is grounded in clinically verified threshold values [13, 15, 80] and encompasses the most typical fall scenarios, ensuring high clinical relevance and practical reproducibility [72, 88, 91]. The selected height thresholds are: 0; 0.1; 0.5; 0.75; 1; 2; 4; 6; 10; and 15 meters (***Table 1***).

The proposed scale is visually presented in ***Fig. 2*** (not to scale).

Intensity of overall external mechanical impact – RTA scenario

Determination of h_{eq} in RTAs. Since h_{eq} was adopted as the reference metric, for falls $h_{eq} = h$. For RTAs (the second most frequent cause of vertebral trauma), recalculation through Δv—the change in the victim's velocity at the moment of RTA—is required [5, 92, 93]. The fundamental concept is that h_{eq} represents the height of free fall that would generate the same kinetic energy as the described RTA [94]. Based on the principle of energy equivalence:

$$\frac{1}{2}m(\Delta v)^2 = mgh_{eq} \Rightarrow h_{eq} = \frac{(\Delta v)^2}{2g},$$

where g=9.81 m/s².

For practical purposes, if Δv is expressed in km/h:

$$h_{eq}\,[m] = \frac{(\Delta v[km/h])^2}{254}.$$

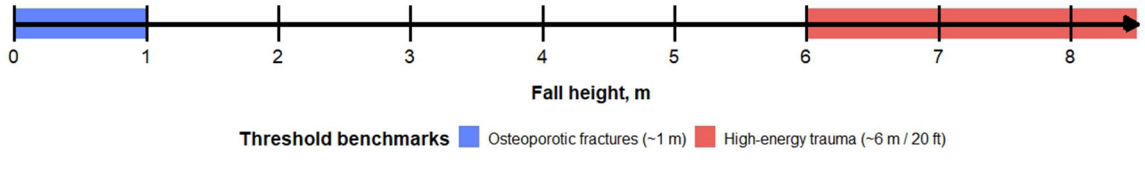

Fig. 1. Currently accepted scale for grading fall height in the context of spinal injury

Table 1. Height-based scale of mechanical exposure intensity (for clinical stratification)

Severity score	Height, m	Clinical scenario
0	0	Absence of external mechanical impact: spontaneous vertebral body compression in severe osteoporosis; fracture under minimal load in the setting of systemic/local bone pathology (tumor, infection, etc.)
1	0–0.1	Incomplete fall/stepwise level change ≤30 cm: stumbling on a flat surface with recovery of balance; partial "sliding" from a step/threshold; microtrauma during an awkward turn in confined space (domestic injury)
2	0.1–0.5	Fall from low furniture or architectural elements ~0.4–0.6 m (low stool, threshold, windowsill); fall from a low bed; in children—fall from a sofa/play surface of comparable height
3	0.50–0.75	Fall from sitting height: from a chair/bed (~0.6–0.7 m); fall during entry/exit from a bathtub; slip while attempting to reach an object from an upper shelf while standing on a seat
4	0.75–1.00	Fall from standing height (~0.8–1.0 m): slipping on ice/wet tiles; tripping over an obstacle (threshold, cable); syncopal fall in upright position; fall while ascending/descending stairs "skipping" a step
5	1–2	Fall from a ladder (2–3 rungs, ~1.5–2.0 m); from a first-floor balcony/platform (<3 m); occupational injury: fall while working on low scaffolding/loading platform; sports-related: fall from a low rock ledge
6	2–4	Fall from the roof of a single-story building (3–4 m), tree, warehouse rack; fall down a significant stair flight (≥6–8 steps); occupational: fall from a ramp/semitrailer
7	4–6	Fall from the second floor (~6 m); from an intermediate landing; fall into a shallow shaft; occupational: fall from an upper tier of construction scaffolding
8	6–10	Fall from the third floor (~9–10 m); from the roof of an industrial hangar/workshop; recreational/occupational fall due to safety failure (impact onto a horizontal surface)
9	10–15	Fall from the fourth–fifth floor (~13–15 m); from a communication mast, crane boom, high scaffolding; fall on a mountain route with impact against ledges/edges during descent
10	>15	Catastrophic fall: height >15 m (≥6th–7th floor); from a high-rise building/antenna mast; fall from a rock cornice/bridge in an urban or mountainous environment

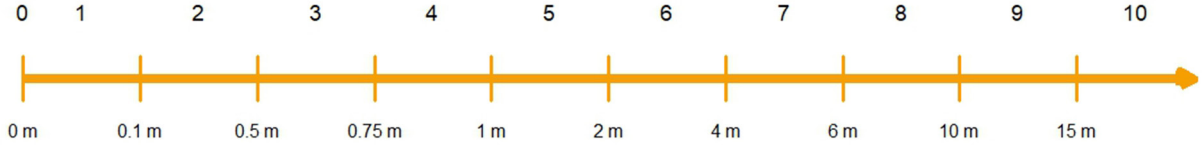

Fig. 2. Level scale (0–10) with boundaries defined by equivalent fall height (heq, m)

Objective limitations in applying this criterion.

First, accurate determination of *Δv* is currently feasible only when data from the vehicle's Event Data Recorder (EDR) (airbag control unit/telematics module) are available. This device records longitudinal and lateral changes in velocity, as well as their resultant value, during the first 0.3 seconds following impact. In the United States, the implementation and standardization of EDR are regulated by the National Highway Traffic Safety Administration (NHTSA), while in the European Union they are governed by Regulation (EU) 2019/2144, which mandated EDR installation in new vehicle models between 2022 and 2024 [95, 96]. Second, even when such equipment is formally present in the vehicle, these data are typically unavailable to the physician during hospital admission and primary assessment. Clinicians are therefore compelled to rely on information obtained from the patient or witnesses [97]. For this reason, indirect methods for estimating *Δv* in various types of RTAs are presented below.

As an example, we provide a detailed method for calculating *Δv* in the case of a collinear one-dimensional collision—that is, a scenario in which both vehicles move along the same straight line (rear-end or head-on collision) and impact occurs strictly along this axis [98].

Let m_1 and m_2 denote vehicle masses; v_1 and v_2 their pre-impact velocities (with signs defined along a single axis); v'_1 and v'_2 their post-impact velocities; and e the coefficient of restitution (typically for vehicles e ≈ 0.0–0.2; discussed in detail below). The derivation is based on the law of conservation of momentum:

$$m_1 v_1 + m_2 v_2 = m_1 v'_1 + m_2 v'_2,$$

and the restitution condition:

$$v'_2 - v'_1 = -e(v_2 - v_1)$$

Solving for the post-impact velocities:

$$v'_1 = \frac{m_1 - em_2}{m_1 + m_2} v_1 + \frac{(1+e)m_2}{m_1 + m_2} v_2$$

$$v'_2 = \frac{(1+e)m_1}{m_1+m_2} v_1 + \frac{m_2 - em_1}{m_1+m_2} v_2.$$

Since $\Delta v = v - v'$, for each vehicle:

$$\Delta v_1 = \frac{(1+e)m_2}{m_1+m_2}(v_1 - v_2),$$
$$\Delta v_2 = \frac{(1+e)m_1}{m_1+m_2}(v_2 - v_1).$$

These expressions demonstrate that each vehicle acquires a fraction of the relative velocity $V_{rel}=|v_1-v_2|$, proportional to the mass of the opposing vehicle. When the masses are equal, each vehicle experiences approximately $\Delta v \approx 0{,}5\,V_{rel}$. If one vehicle is substantially heavier ($m_2 \gg m_1$),the lighter vehicle "absorbs" nearly the entire relative velocity change ($\Delta v_1 \rightarrow (1+e)V_{rel}$), whereas the heavier vehicle undergoes minimal velocity change ($\Delta v_2 \approx 0$).

Since, in the above calculations, the coefficient of restitution is a parameter that is difficult to assess empirically, its brief characterization is provided below. In mechanics, e is defined as the ratio of the relative separation velocity to the relative approach velocity of colliding bodies along the line of impact [99, 100], i.e.:

$$e = \frac{v_2' - v_1'}{v_1 - v_2}.$$

Its values may be interpreted as follows:

$e=0$ — perfectly inelastic collision: after impact, the bodies move together as a single unit, and their common velocity v' is determined by the law of conservation of momentum [101];

$0<e<1$ — partially elastic collision: a portion of the relative velocity is preserved as "rebound" [102]

$e=1$ — perfectly elastic collision: kinetic energy is fully conserved (as in ideally rigid bodies, e.g., a billiard ball) [103, 104].

Vehicle bodies and bumpers are engineered to maximize energy absorption through plastic deformation during impact [105, 106]. Consequently, most motor vehicle collisions are predominantly plastic in nature. For this reason, the coefficient of restitution e in real-world RTAs is typically very small. Its value reflects only the fraction of energy retained in elastic deformation and subsequently released as a minor "rebound" effect.

In frontal collisions, e is generally within the range of 0.0–0.1, since nearly all energy is dissipated in structural crumpling [106]. In lateral impacts, the value is slightly higher (0.1–0.2), owing to a smaller programmed deformation zone and a relatively greater elastic response [107]. In low-speed rear-end collisions (bumper-to-bumper, parking scenarios), the coefficient may reach 0.2–0.3, as a greater proportion of elastic components is engaged and plastic deformation is limited. In impacts with rigid obstacles (e.g., a pole or a tree), e approaches zero [99, 107]. For collisions with Δv > 25 km/h, practical calculations conventionally assume e = 0, since the contribution of the elastic component becomes negligible.

To illustrate the practical application of the proposed calculation algorithm, several clinical examples are provided below.

Example 1. Passenger car A overtakes at a speed of v_1 = 90 km/h, while passenger car B approaches from the opposite direction at v_2 = 70 km/h. The collision is frontal and aligned with the direction of motion. Let m_1 = 1400 kg and m_2 = 1300 kg. Taking into account the impact severity, the coefficient of restitution is assumed to be e = 0. Accordingly, $V_{rel}=V_1+V_2=160$ km/h, $m_1+m_2=2700$ kg.

$$\Delta v_1 = \frac{m_2}{m_1+m_2}V_{rel} \approx 77\ km/h,$$
$$\Delta v_2 = \frac{m_1}{m_1+m_2}V_{rel} \approx 83\ km/h.$$

The equivalent fall height h_{eq} (based on Δv) is therefore:

$$h_{eq.1} \approx \frac{77^2}{254} \approx 23.4\,m,$$
$$h_{eq.2} \approx \frac{83^2}{254} \approx 27.1\,m,$$

For both affected vehicles, this corresponds to the maximum level of mechanical impact on the human body—10 points according to the proposed scale.

Example 2. Passenger car A, traveling at v_1 = 50 km/h, collides with passenger car B, which is stationary at a traffic light. In this case, the vehicle masses are assumed equal: $m_1=m_2=1400$ kg.

With e=0

$$\Delta v_1 = \Delta v_2 = \frac{1}{2}\,50 = 25\ km/h$$

$$h_{eq.1} = h_{eq.2}\ \frac{25^2}{254} \approx 2.46\,m,$$

which corresponds to 6 points on the proposed scale.

A logical objection to the use of the proposed methodology is the difficulty of accurately determining vehicle speed at the time of a RTA. However, in practical settings, drivers are generally able to provide an approximate estimate sufficient for primary stratification. To demonstrate the robustness of the conclusions with respect to plausible speed estimation error, several representative calculations based on Example 2 are presented below:

- 50 km/h→ Δv=25.0 km/h→ h_{eq}=2.46 m → 6 points;
- 55 km/h→ Δv=27.5 km/h→ h_{eq}=2.98 m → 6 points;
- 60 km/h→ Δv=30.0 km/h→ h_{eq}=3.54 m → 6 points.

These results demonstrate that moderate uncertainty in the initial speed does not alter the clinical assessment category. Furthermore, analysis indicates that, in calculating the equivalent fall height, small differences in vehicle mass (±100–200 kg) have a negligible effect on the resulting Δv and, consequently, do not influence classification according to the proposed scale. In clinical practice, such fine-grained precision is unnecessary. Of substantially greater importance is the vehicle class (e.g., subcompact car, sedan, SUV/crossover, minivan, truck, bus, articulated heavy truck), as inter-category differences are considerable and may significantly affect the distribution of impact severity between collision participants. Therefore, for stratification purposes, classification by vehicle type provides sufficient accuracy while preserving the practical applicability of the method. When vehicle masses are approximately equal, Δv equals one-half of the total closing speed, irrespective of the exact masses; thus, a coefficient of 0.5 is used in calculations.

Analogously to the section on colinear (1D) collisions, simplified coefficients for rapid estimation of Δ*v* in other types of RTAs were derived using methods of formal mechanics. These coefficients allow prompt estimation of the change in velocity of the injured vehicle—and subsequent calculation of h_{eq} —based solely on the speed of one participant and the collision configuration (***Table 2***).

When analyzing the table, particular attention should be paid to the rollover category of RTAs, which fundamentally differs from other scenarios in terms of Δ*v* determination. In this case, the change in velocity is not directly related to the frontal or lateral projection of the relative velocity but is determined by the characteristics of the vehicle's rotational motion and the number of body contacts with the surface [113]. A basic estimate is performed using the formula:

$$\Delta V_{roll} \approx k_{roll} \cdot V_0$$

where V_0 — is the velocity prior to the onset of rollover; k_{roll} — is a coefficient dependent on the number of rollovers/roof contacts, the rollover type, and the environmental conditions.

In the analysis of rollover RTAs, several methods are used to determine Δ*v*, two of which are considered the simplest and most effective. Both approaches are conceptually equivalent. It is recommended to apply the method that is easier to interpret based on the available documentation:

1. Quarter-turn (Nq) estimation method [114]. The assessment is based on the number of quarter-turns of the vehicle body (90° rotation = 1 quarter-turn):

Nq=1-2 – the vehicle comes to rest on its side or roof: k_{roll} ≈0.25–0.35;

Nq=3–4 – rollover over the roof or a complete 360° rotation: k_{roll} ≈0.35–0.50;

Nq ≥ 5 – multiple rollovers: k_{roll} ≈0.50–0.65.

2. Roof-impact count method (M, roof impacts) [115–117]. This method estimates the number of roof or pillar contacts with the road surface and is particularly convenient in cases of multiple rollovers:

$$k_{roll} \approx 0.2 + 0.08 \cdot M$$

where *M* is the number of contacts. In practice, k_{roll} does not exceed 0.65. To improve calculation accuracy, contextual adjustments are recommended depending on the specific conditions [113. 118]. In the analysis of rollover RTAs, the following scenarios are distinguished:

- "Tripped" rollover, initiated by an external obstacle (e.g., curb, ditch, soft shoulder) that "catches" the wheel and triggers rotation. Such scenarios are more likely to result in abrupt energy dissipation and a greater Δ*v*. In calculations: k_{roll} +0.03–0.05;

- "Untripped" rollover, occurring due to the vehicle's own dynamics (sharp maneuver, skidding, center-of-gravity displacement) without impact against an external obstacle. In these cases, Δ*v* is usually lower than in "tripped" scenarios; therefore, the coefficient is adjusted downward: k_{roll} –0.03…–0.05.

Additionally, terrain and surface conditions are taken into account: steep slope/embankment (k_{roll} =+0.03) hard road surface (asphalt) – k_{roll} –0.02…–0.03, soft surface (soil)– k_{roll} +0.02–0.03 [119]. Example. A vehicle was traveling on a rural road at approximately 70 km/h. During an overtaking maneuver, one wheel entered a soft unpaved shoulder. Loss of support caused a "tripped" rollover (a typical obstacle-initiated rollover), after which the vehicle overturned laterally, making two roof contacts with the surface.

Using the roof-impact method with M=2 k_{roll}≈0.36. Since the rollover was initiated by "tripping" on a soft soil edge, corrections of +0.04 ("tripped" mechanism) and +0.02 (soil surface) are applied, yielding a final: k_{roll} ≈0.42.

Thus,

$$\Delta v \approx (0.36 + 0.04 + 0.02) \cdot V_0 \approx 0.42 \cdot 70 \approx 29.4\ km/h$$

$$h_{eq} \approx \frac{29.4^2}{254} \approx 3.4\ m$$

The obtained value corresponds to level 6 on the proposed scale (interval 2–4 m).

Table 2. Coefficients for rapid estimation of Δv in various types of RTAs (assuming comparable vehicle masses) [107–112]

Type of RTA	Coefficient (k) for Δv	Comment
Colinear (frontal/ rear-end)	0.5	Each vehicle receives half of the relative velocity
Lateral impact	0.5	For the struck vehicle, Δv ≈ half of the normal velocity component
Oblique impact	0.25 – for 30⁰ 0.35 – for 45⁰ 0.43 – for 60⁰ 0.48 – for 75⁰	Δv depends on the contact angle
Sideswipe	0.05–0.20	With tangential contact, Δv is small; energy is dissipated in friction/sliding
Impact with rigid barrier	≈1	With e ≈ 0, Δv approximates the impact speed
Rollover	0.25–0.65	Δv estimated as a fraction of pre-rollover speed; depends on number of rotations
Multi-event collision	Maximum Δv	In multiple impacts, the largest Δv is used (based on EDR data or reconstruction)

The presented data demonstrate the feasibility of applying relatively simple methodologies for approximate assessment of the traumatic mechanical impact on the human body within two fundamental scenarios—fall from height and various types of RTAs. To accelerate and simplify information processing, eliminate the need for independent mathematical calculations, and account for multiple modifying factors, we developed a dedicated online calculator. Its structure, functional capabilities, and operating algorithms are described in the corresponding section of this article.

Assessment of mechanical impact on the spine

It is evident that h_{eq}, which reflects only the integrated magnitude of mechanical exposure, alone does not allow an adequate assessment of the impact on the spine [70]. Actual traumatic potential is determined by how the energy is converted into forces over the duration of deceleration and along the deceleration path, the geometry of its application to the body, and the proportion that mechanically affects the spinal column [1, 120]. Therefore, identical h_{eq} values can correspond to fundamentally different clinical outcomes [77, 121, 122]. For example, a fall from 1 m onto rigid concrete versus a thick mat, even with identical h_{eq}, results in markedly different loading and risk of injury [123].

Key additional factors influencing actual traumatic potential include the patient's body mass, the impulse transfer coefficient, and the effective deceleration distance [120, 124–126].

Patient body mass

The patient's body mass (m) is a fundamental parameter that determines the inertial properties of the system [127, 128]. For any traumatic event with a given Δv, and consequently a given equivalent height h_{eq}, mass linearly scales both the energy to be dissipated and the impulse that must be absorbed by supporting structures [129, 130].

According to the integral form of Newton's second law, the work of external forces required to bring the body to a complete stop equals its kinetic energy (E):

$$E = \frac{1}{2}m(\Delta v)^2 = mgh_{eq}.$$

At fixed V or h_{eq} the energy E is proportional to mass. Thus, a heavier body requires dissipation of a greater energy reserve at the same h_{eq}.

The impulse (J) that braking forces must provide is calculated as:

$$J = \int F(t)dt = m\Delta v$$

Impulse increases linearly with mass at a fixed Δv [131]. Accordingly, if the deceleration occurs over a fixed time (t), the average applied force is:

$$\bar{F} = \frac{J}{t} = \frac{m\Delta v}{t}$$

which also scales linearly with mass.

Closer to clinical practice, the relevant scenario is deceleration over a characteristic path (s), e.g., the thickness of a cushioning surface or the deformation depth of a structure. In this case, the average applied force can be calculated as:

$$\bar{F} = \frac{E}{s} = \frac{mgh_{eq}}{s},$$

which similarly reflects a linear dependence on mass under otherwise identical conditions [132, 133].

Thus, patient body mass is an independent modifying factor for traumatic potential. At fixed Δv or h_{eq}, it systematically increases the impulse and work required to stop the body, and consequently the average and peak loads transmitted to the spinal supporting structures [125]. For a correct interpretation of "event force," body mass should be considered at least descriptively, even if the metric used for assessment is mass-neutral [134].

Impulse transfer coefficient

The impulse transfer coefficient (T_{land}) is a dimensionless quantity that characterizes the fraction of mechanical energy from a traumatic event that reaches the spine [1, 135]. It reflects the effectiveness of "biomechanical filters" (joints, muscles, soft tissues) and protective systems (seat belts, airbags, seats) that dissipate or redistribute the impact [120, 136]. Accordingly, T_{land} determines the portion of the total mechanical exposure that is transformed into loading on the spinal column. While axial compression is most common, other components (shear or rotational) may dominate depending on the direction and resultant vector of the applied force [137].

The primary factors influencing T_{land} are the point of force application and contact geometry [126, 137, 138]. For instance, a fall onto the feet with deep knee flexion and active muscular engagement dissipates a significant portion of the impulse, yielding $T_{land} \approx 0.4–0.6$ [139, 140]. Conversely, a fall onto the buttocks or back results in minimal absorption, with T_{land} approaching 0.9–1.0, transferring almost the entire energy to the thoracolumbar spine [141]. In frontal RTAs, seat belts and airbags distribute the kinetic load across the chest and shoulder girdle, increasing the area and duration of energy absorption, thereby reducing direct impulse transfer to the spine [142, 143]. In the absence of restraints, impact against the steering wheel or dashboard occurs locally, with negligible damping, transmitting almost the entire load to the spinal column. In some cases (e.g., axial head impact), local impulse concentration may formally exceed 1, reflecting not "energy generation" but amplification of its effect on a limited spinal segment [144].

In clinical practice, T_{land} is estimated based on the injury scenario: which structures bear the main load, how much energy is absorbed along the transmission path, and what fraction reaches the spinal column [126, 141]. For calculations, a typical (average) coefficient value is used, while minimum and maximum limits are considered as a variability range.

Based on literature analysis, average T_{land} values with approximate ranges have been determined for main clinical scenarios (***Table 3***).

Table 3. Average impulse transfer coefficient values for the thoracolumbar spine in common clinical scenarios [1, 70, 120, 126, 135–154]

Brief description	Tland (min–typical–max)	Justification (concise)
Falls:		
Onto feet, deep absorption (deep squat)	0.40–0.55–0.65	Significant portion of the impulse is dissipated through knee and hip joint flexion and the musculoskeletal complex; no more than half of the energy reaches the spine
Onto feet, semi-flexed	0.60–0.70–0.80	Moderate energy filtering through joints and muscles; axial load fraction transmitted is higher than in deep absorption, but part of the impulse is absorbed
Onto feet, stiff/almost locked	0.80–0.90–0.95	Minimal joint cushioning; impulse is almost fully transmitted along the spinal axis, generating marked compression
Onto buttocks/pelvis	0.80–0.95–1.05	Limited cushioning by soft tissues of the pelvis; load is almost entirely transmitted to the lumbar spine. Local concentration (>1) may occur in some cases
Onto back	0.90–1.05–1.15	Impact over a broad surface with transmission through the rib-spine framework produces nearly complete axial loading; additional bending moment may occur
Onto side/pelvis	0.60–0.75–0.85	Significant portion of energy dissipated through lateral soft tissues and pelvic structure; axial component reduced
Onto hands/elbows/knees	0.40–0.60–0.70	Extremities act as shock absorbers, dissipating part of the energy; only 40–70% of impulse reaches the spine
Onto knees (with subsequent axial impact)	0.50–0.70–0.85	Primary filtering through knee flexion, followed by sharp transmission of residual energy along the axis; final fraction is variable
RTAs:		
Frontal, seatbelt + airbag	0.50–0.65–0.75	Seatbelt and airbag distribute load across the chest and shoulder girdle, prolonging contact duration and reducing the fraction of energy transmitted to the spine
Frontal, seatbelt only	0.60–0.75–0.85	Without an airbag, load distribution is less effective; impulse through the belt and chest is largely transmitted to the spine
Frontal, no restraint (dashboard/steering wheel)	0.85–0.95–1.00	Direct chest contact with steering wheel or panel; absence of cushioning structures leads to almost full impulse transfer to the spine
Side impact, with seatbelt	0.55–0.70–0.80	Belt restrains the torso and redistributes part of the energy; door and seat deformation further dissipate load
Side impact, no seatbelt	0.70–0.85–0.95	Rigid impact through lateral body surface; absence of controlled distribution increases transmitted fraction
Rollover, with seatbelt	0.90–1.00–1.10	Roof contact with head/shoulders generates axial load with minimal filtering; local concentration can increase transmission
Rollover, no seatbelt	0.90–1.05–1.15	Contact with rigid cabin elements or ground; impact geometry is variable, but direct, localized loading on the spine is more frequent

Note: For practical calculations, it is recommended to use the typical (average) Tland value, as it represents the most probable contact scenario. The "min" and "max" values are provided as references to assess the degree of variability and potential calculation error.

Effective deceleration distance

The effective deceleration distance (S_{land}) is defined as the actual path over which the velocity of the body (or the spine-relevant portion of it) is reduced following an impact [139, 150]. Unlike the "geometric" fall height, S_{land} encompasses all sources of system "compliance": support deformation (mats, soil, seats, airbags), soft tissue compression, joint flexion, as well as body sliding and rotation [129, 133]. A greater S_{land} distributes energy absorption more smoothly over time, resulting in lower average and peak spinal loads for the same event [154].

Factors influencing S_{land} include the point of force application and body posture (e.g., legs with flexed knees provide a long deceleration path, whereas landing on the buttocks or back yields a short path), surface properties (rigid asphalt offers minimal energy absorption, whereas soft surfaces, snow, or mats extend the deceleration distance), and passive safety elements in vehicles (seatbelts, pretensioners, airbags, seat and chassis deformation increase the effective path) [152] (***Tables 4 and 5***). Secondary movements are also important: sliding, rolling, and rotation reduce strictly axial compression on the spine, effectively increasing the deceleration distance [113, 118].

In clinical practice, the assessment is performed according to the scenario and context: body position at the moment of contact, surface or equipment type, and the nature of the injuries are analyzed, after which a realistic range of values is selected for calculations.

Proposed metrics for injury characterization

Based on the analysis of the described parameters and the principles of applied mechanics, a set of metrics has been proposed to formalize and quantitatively describe the mechanical impact on the spine.

Table 4. Effective deceleration distance values for selected typical clinical scenarios [131, 136, 139–150, 152–154]

Brief description	*Sland, m (min–typical –max)*	Mechanism
Falls:		
Onto feet, deep absorption (deep squat)	0.40–0.50–0.60	Knee and hip flexion, foot elasticity, posterior pelvic shift
Onto feet, semi-flexed	0.25–0.30–0.40	Partial knee flexion, joint elasticity, moderate absorption
Onto feet, stiff/almost locked	0.15–0.20–0.25	Minimal joint motion, abrupt impact transmission; short path
Onto buttocks/pelvis	0.02–0.04–0.06	Soft tissue compression, minimal sliding; very short path
Onto back	0.03–0.04–0.05	Deformation of back and chest soft tissues upon impact
Onto side/pelvis	0.06–0.08–0.10	Lateral soft tissue deformation and pelvic compression
Onto hands/elbows/knees (with load transfer)	0.10–0.15–0.20	Limb flexion, partial energy absorption by joints
Onto knees (with subsequent axial impact)	0.08–0.10–0.12	Soft tissue compression of the knees + joint flexion before spinal impact
RTAs:		
Frontal: seatbelt + airbag	0.20–0.30–0.40	Belt stretch, airbag compression, seat deformation
Frontal: seatbelt only	0.15–0.25–0.30	Belt elongation and seat deformation
Frontal: no seatbelt (dashboard/ steering wheel)	0.02–0.05–0.08	Near-instantaneous stop; extremely rigid contact
Side impact, with seatbelt	0.10–0.15–0.25	Door/seat deformation, torso sliding
Side impact, no seatbelt	0.05–0.10–0.15	Rigid contact; minimal controlled deformation
Rollover, with seatbelt	0.02–0.04–0.08	Roof contact with head/shoulders; limited deceleration path
Rollover, no seatbelt (contact with cabin/ground)	0.02–0.06–0.10	Rigid, variable geometry; short deceleration distance

Note: For practical calculations, it is recommended to use the typical (average) Sland value, as it represents the most probable contact scenario. The "min" and "max" values serve as references to estimate variability and potential calculation error.

Table 5. Modification factors for effective deceleration distance depending on environment, surface, and equipment [123, 155–168]

Parameter	Contribution to Sland, m (min– typical–max)
Asphalt/concrete/tiles	0.001–0.003–0.005
Wooden floor/linoleum	0.002–0.005–0.010
Sports mat 10–20 mm thick	0.01–0.02–0.03
Tatami mat 40–60 mm thick	0.03–0.05–0.07
Gymnastics mat 80–120 mm thick	0.08–0.12–0.18
Compacted soil/ground	0.005–0.015–0.030
Dry sand (beach)	0.10–0.20–0.30
Wet/compact sand	0.05–0.10–0.20
Packed snow	0.02–0.05–0.10
Loose snow (20–40 cm)	0.15–0.30–0.50
Water, entry "feet first"	0.50–1.00–1.50
Water, entry "flat"	0.05–0.10–0.20
Light clothing	0.002–0.005–0.010
Winter/multilayer clothing	0.01–0.02–0.03

Note: when modification factors are considered, the calculation uses the sum of the relevant components along the load path.

1. Mean "spinal" overload

The mean spinal overload ($\bar{g}_{spine}$) reflects the "stiffness" of the injurious event's impact on the spine and is expressed in multiples of gravitational acceleration (g). Unlike absolute force or energy parameters, ($\bar{g}_{spine}$) is independent of the patient's body mass and therefore provides a universal, comparable criterion across different clinical scenarios [169].

Formally, it is defined as:

$$\bar{g}_{spine} = \frac{h_{eq}}{S_{land}} * T_{land}.$$

For falls, $\bar{g}_{spine}$ is primarily determined by surface type and body position: minimal deceleration distance (e.g., falling on asphalt or concrete) results in high overloads, whereas soft ground, water, or mats increase the deceleration distance and reduce overload [133, 152, 170]. When falling on the feet, overload depends on the ability to absorb impact: the deeper the joint flexion, the longer S_{land} and the lower $\bar{g}_{spine}$.

In RTAs, the indicator depends on the effectiveness of passive safety systems. Seat belts and airbags increase the deceleration distance and duration, distribute the load over a larger area, and reduce the net overload [143, 170, 171]. In the absence of restraint systems or during contact with rigid cabin structures, deceleration distance is minimal, T_{land} approaches 1, and $\bar{g}_{spine}$ reaches maximum values.

The main advantage of $\bar{g}_{spine}$ is its comparability: the same value indicates the same "stiffness" of spinal loading regardless of the victim's body mass [169]. It is assumed that this metric correlates well with the probability of structural injuries and can serve as a key integrative criterion of biomechanical trauma.

2. Energy acting on the spine

The energy acting on the spine (E_{spine}) quantifies the absolute amount of mechanical energy absorbed by the spinal column. Unlike mass-neutral metrics, which reflect relative "stiffness" of impact, E_{spine} indicates the full energy budget that the spine must absorb:

$$E_{spine} = m\ g\ h_{eq}\ T_{land}$$

For falls, E_{spine} primarily depends on body mass and the biomechanical load path: when falling on the "feet", part of the energy is absorbed by joints and muscles, whereas when falling on the buttocks or head, nearly the entire impulse is transmitted along the spinal axis [158, 172, 173]. In RTAs, the energy reaching the spine depends on passenger mass and the force direction (through the chest or pelvis) [174]. Passive safety systems (belts, airbags) do not reduce E_{spine} but increase S_{land}, spreading the impulse over time and reducing peak loads [175, 176].

The advantage of this metric is its physical transparency: it is expressed in absolute energy units (J) and can be used for engineering and biomechanical calculations, as well as injury modeling. Its limitation is mass dependence: for the same h_{eq}, a heavier patient inevitably experiences a greater energy load on the spine [177].

Thus, E_{spine} should be considered a secondary parameter, important for analyzing the total energy component of an event and for biomechanical modeling, whereas mass-neutral metrics may be preferable for clinical comparison.

3. Mean force acting on the spine

The mean force acting on the spine ($\bar{F}_{spine}$) represents the averaged magnitude of the axial force transmitted to the spine during deceleration. Unlike mass-neutral parameters, F_{spine} directly depends on the patient's body mass and therefore characterizes the absolute force scale of the traumatic impact.

$$\bar{F}_{spine} = \frac{m\ g\ h_{eq}\ T_{land}}{S_{land}}$$

In falls, the magnitude of is determined by body mass and the type of contact: falling onto a rigid surface with minimal deceleration distance leads to extremely high mean forces [161, 162], whereas soft surfaces or the shock-absorbing properties of the joints substantially reduce them [155, 167]. In traffic collisions, the parameter depends on passenger body mass and the effectiveness of restraint systems [176]. Seat belts and airbags increase S_{land}, thereby reducing both mean and peak forces [178].

The advantage of this metric lies in its intuitive clarity: force expressed in newtons is readily interpretable for clinicians and engineers and can be directly compared with known strength limits of osseoligamentous structures [173]. Its limitations include dependence on body mass and the difficulty of accurately estimating S_{land}. Moreover, in real-world conditions, the peak force—rather than the mean force—may be most critical and may differ substantially from the averaged value [177].

Thus, $\bar{F}_{spine}$ may be regarded as an additional force descriptor useful for engineering and biomechanical applications, but not as a primary clinical indicator.

4. Spinal-equivalent height

The spinal-equivalent height (h_{spine}^{eff}) – is a recalculated (normalized) equivalent fall height that would produce the same mean axial load on the spinal column under reference deceleration conditions as the actual traumatic event under its specific posture and contact characteristics. This metric is mass-neutral and therefore enables valid case comparisons. The concept is to reduce heterogeneous injury mechanisms to a single, physically interpretable "height" scale specifically oriented to the spine, taking into account load transmission and contact "stiffness." Formally, it is defined as:

$$h_{spine}^{eff} = h_{eq}\ \frac{s_{ref}}{s_{land}}\ T_{land},$$

where s_{ref} – is the reference deceleration distance (0.10 m in the present study).

In clinical fall scenarios the magnitude of h_{spine}^{eff} naturally differentiates contact regimes. When landing on the feet, S_{land} is large due to multijoint shock absorption (knee and hip flexion, footwear elasticity), and part of the impulse and work is dissipated distal to the spine. This is reflected in a reduced transmission coefficient T_{land} (<1). Conversely, when falling onto the back or buttocks, the deceleration distance is markedly shorter (rigid contact, minimal support deformation), the axial impulse component is maximal, T_{land} increases, and for the same

h_{eq} a greater h_{spine}^{eff}, is obtained—indicating a locally "stiffer" impact on the thoracolumbar spine [172, 173]. In traffic collisions, the metric reflects the performance of passive safety systems: seat belts, pretensioners, and airbags do not alter the total energy budget of the event (mgh_{eq}), but they increase S_{land} (by extending torso deceleration distance and spreading the impulse over time), thereby reducing h_{spine}^{eff} [175, 176]. The geometry of the load path (through the torso) generally remains unchanged; thus, in first approximation, T_{lan} varies minimally.

Fixing the reference distance at s_{ref}=0.1 m standardizes the metric and ensures comparability across scenarios: h_{spine}^{eff} should be interpreted as the "height under standard conditions" energetically equivalent to the given event specifically for the spine. As noted above, the mean axial spinal overload in units of g is:

$$\bar{g}_{spine} = \frac{h_{eq}}{S_{land}} * T_{land} \Rightarrow \bar{g}_{spine} = \frac{h_{spine}^{eff}}{s_{ref}}.$$

In other words, h_{spine}^{eff} represents the mean spinal deceleration $\bar{g}_{spine}$ converted into "meters" relative to the selected s_{ref}, thereby preserving the physical relationship with deceleration dynamics while simultaneously providing an intuitive clinical interpretation [179]. The metric is mass-neutral and therefore suitable for population-based comparisons and for correlation with indicators of bone tissue quality.

The principal advantage of this parameter lies in the unification of event force description within a convenient "height-based" format while maintaining spine-specific clinical relevance. This facilitates risk stratification and cohort comparison, enables the direct conversion of h_{spine}^{eff} into categorical scores of the proposed (spine-oriented) scale for operational communication and statistical analysis, and allows its application in constructing quantitative associations with bone quality indicators—dual-energy X-ray absorptiometry (DXA), trabecular bone score (TBS), and computed tomography–derived density expressed in Hounsfield Units (CT-HU) [180, 181].

The limitations of the metric are related to the need for expert reconstruction of contact conditions: errors in the estimation of S_{land} and T_{land} are linearly propagated into the final result. Therefore, detailed documentation of injury circumstances substantially enhances the accuracy and effectiveness of the assessment.

Overall, h_{spine}^{eff} serves as a fundamental mass-neutral descriptor of mechanical exposure to the spine, integrating event geometry, posture, deceleration path, and the point of force application, thereby ensuring a physically valid and clinically meaningful evaluation of impact severity.

Development of the online calculator

To accelerate data processing, eliminate the need for constant reference to lookup tables, expand the range of applicable scenarios, and simplify coefficient adjustment for validation purposes, we developed a web-based calculator (***Fig. 3***).

The tool provides modular input based on typical scenarios ("Fall," "RTA"), automatically populating standard values and ranges for the parameters T_{land} and S_{land} depending on the selected body position and landing surface. In the case of RTAs, it additionally supplies rapid estimation coefficients for Δ*v* according to vehicle

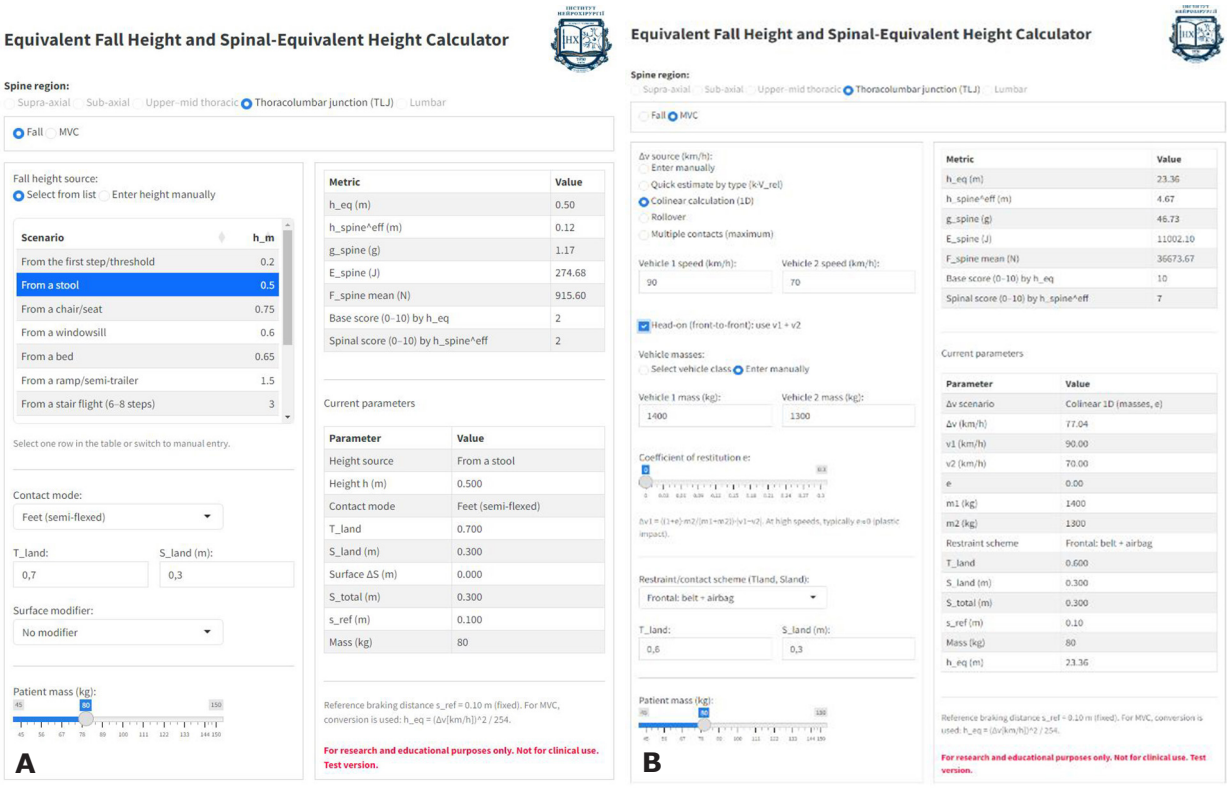

Fig. 3. Interface of the developed web calculator: A — fall; B — RTA

type and collision pattern. Users may retain the "default values" (in accordance with the embedded reference libraries) or manually override them; all modifications are instantly incorporated into the calculations.

The calculator is available at: www.spine.org.ua/scale.

Validation of the scale and derived metrics

The objective of the subsequent phase was to quantitatively evaluate the metric properties of the spine-oriented measure h_{spine}^{eff} and its derived indicators (baseline h_{eq}, $\bar{g}_{spine}$, E_{spine} and $\bar{F}_{spine}$), as well as the final composite scores (0–10) based on these parameters. The analysis included assessment of construct and criterion validity, relative and absolute reliability, agreement for continuous metrics, threshold stability, and known-groups validity.

Construct validity. Within the dataset of clinical and anamnestic variables used for verification, the metric h_{spine}^{eff} demonstrated the expected convergence with the integral measure of mechanical exposure: the correlation with baseline h_{eq} was 0.82 ($p < 0.001$), indicating that approximately 67% of the variance in h_{spine}^{eff} is explained by variability in event energy normalized to height. Associations with spinal injury morphology based on CT/MRI findings were also consistent with theoretical expectations: increasing h_{spine}^{eff} was accompanied by greater anterior wedge deformation ($r = 0.58$, $p < 0.001$; explained variance ≈34%) and a higher degree of spinal canal compromise ($r = 0.49$, $p < 0.001$; explained variance ≈24%). A monotonic relationship was identified with ordinal injury severity according to the AO Spine classification ($\rho = 0.62$, $p < 0.001$): progression from low-energy patterns (A1) to burst and complex types (A3/A4, B/C) was associated with increasing metric values.

In binary logistic regression for the threshold ≥A3, each additional 1 m was associated with a 1.85-fold increase in the odds ratio (OR) of sustaining burst/unstable injuries (95% CI 1.45–2.38, $p < 0.001$), after adjustment for age and sex. This finding is consistent with the biomechanical interpretation of the metric: an increase of 1 m in h_{spine}^{eff} nearly doubles the odds of injuries classified as ≥A3.

From a practical standpoint: if at h_{spine}^{eff} = 0.8 m the conditional probability of injury ≥A3 is approximately 20% (OR ≈0.25), then at 1.8 m (+1 m), the OR increases by a factor of 1.85 (≈0.46), and the probability rises to approximately 32%; with a 2 m increase, it approaches ≈46%. Assessment of logit linearity (Box–Tidwell test, restricted cubic splines) revealed no significant nonlinearity within the studied range and no evidence of multicollinearity.

The mass-neutral property, which is critically important for this metric, was confirmed by partial correlation with body weight: after controlling for mechanism and position, $r = 0.06$ ($p = 0.41$), indicating no statistically significant association. In contrast, the energy-dependent metric E_{spine} showed the expected strong correlation with body mass ($r = 0.74$, $p < 0.001$). These results support the theoretical interpretation of h_{spine}^{eff} as an indicator of external mechanical exposure to the spine rather than a surrogate marker of bone tissue strength.

Criterion validity. In the absence of external verified indicators (EDR, objective measurement of height), clinical outcomes based on neuroimaging findings served as the criterion. The ability of h_{spine}^{eff} to predict the presence of vertebral fracture was rated as "good" according to the Hosmer–Lemeshow criteria: the area under the ROC curve (AUC) was 0.82 (95% CI 0.73–0.90). For the detection of compression–burst injuries (A3/A4), the AUC was 0.78. An optimal threshold of approximately 1.3 m yielded a sensitivity of ≈0.76 and a specificity of ≈0.72 (based on the maximum Youden index). This corresponds to LR^{+}≈2.7 and LR^{-} ≈0.33, which clinically indicates a weak to borderline moderate increase in post-test probability with a positive result and a weak decrease with a negative result. Thus, the metric is useful as an adjunctive tool for risk stratification. For features of posterior ligamentous complex injury, discrimination was predictably lower due to more complex biomechanics: AUC = 0.74, with a threshold of approximately 2.4 m. In screening scenarios (where minimizing missed cases is critical), lowering the threshold below the optimum (favoring sensitivity) is advisable; in confirmatory contexts, raising the threshold above the optimum (favoring specificity) is appropriate. By definition, a single mechanical descriptor cannot account for the full extent of interindividual variability; however, the reported AUC values indicate practically meaningful diagnostic utility for risk stratification and severity ranking.

Additional robustness checks (restriction of analyses to cases with low uncertainty regarding T_{land} and S_{land}, analysis limited to thoroughly documented postures and contact surfaces, and bootstrap estimation of AUC) did not materially alter the conclusions. Model calibration (intercept/slope) remained satisfactory, with no evidence of systematic bias in clinically relevant threshold ranges. Collectively, construct and criterion validity consistently support that h_{spine}^{eff} is an informative indicator of "event severity" for the spine, useful for clinical communication, stratification, and research on associations with bone quality and therapeutic outcomes.

Relative reliability of measurements. Inter-rater agreement for the presented anamnestic cases (n = 40, 5 experts) was assessed using the intraclass correlation coefficient ICC (2.1) (two-way random-effects model, absolute agreement, single measure). For the baseline score calculated directly from h_{eq}, ICC was 0.84 (95% CI 0.77–0.89), corresponding to "good" agreement. For the spine-oriented score based on h_{spine}^{eff}, ICC was slightly lower at 0.79 (95% CI 0.71–0.86), also within the "good" reliability range.

When averaging the ratings of five experts (ICC(2,k)), agreement increased to 0.95 and 0.92 for h_{eq} and h_{spine}^{eff}, respectively, corresponding to an "excellent" level. The weighted κ coefficient with quadratic weights was 0.78 (h_{eq}) and 0.72 (h_{spine}^{eff}), indicating "substantial" agreement according to the scale of Landis & Koch.

Repeated assessment of a subsample of cases (test–retest, 10 cases, reassessment after ≥2 weeks) demonstrated high stability: ICC (2,1) was 0.90 (95% CI 0.83–0.95) for the baseline score and 0.85 (95% CI 0.76–0.92) for the spine-oriented score. The mean absolute difference between the first and repeated assessments

was 0.42 and 0.58 points, respectively, confirming high temporal reproducibility of the instrument.

Absolute reliability. To evaluate the precision of individual measurements, SEM and MDC_{95} were calculated.

$$SEM = SD\sqrt{1 - ICC},$$

where SD is the standard deviation of scores across the entire sample.

For the baseline score, SEM was 0.80 points; for the spine-oriented score, 0.95 points.

MDC_{95}, was calculated as

$$MDC_{95} = 1.96\sqrt{2}\,SEM,$$

yielding ≈2,2 і 2,6 points for h_{eq} and respectively.

These findings indicate that fluctuations of less than 2–3 points may be attributable to random variability. At the same time, the clinical relevance of such differences depends on the scale range: at lower levels (where intervals correspond to tens of centimeters), a change of 1–2 points is usually not meaningful, whereas at higher levels even a 1-point difference (corresponding to an increase in height by an order of meters or tens of meters) may reflect a substantial change in mechanical exposure. In general, exceeding the MDC_{95} threshold of approximately 2–3 points is highly likely to represent a statistically significant difference; however, its clinical interpretation should consider the scale level.

Thus, the scale demonstrates both high relative reliability (inter-rater agreement and temporal stability) and acceptable absolute precision (low SEM and MDC) (***Table 6***). This supports its use both for patient stratification based on a single measurement and for longitudinal monitoring, in which changes ≥MDC should be considered meaningful.

Agreement for continuous metrics. To assess agreement between the calculated metric values (based on expert ratings) and the reference algorithmic computations (online calculator based on author-derived values), Bland–Altman plots were constructed (***Fig. 4***).

Table 6. Indicators of relative and absolute reliability of the scale (40 cases, 5 experts)

Indicator	Baseline score (h_{eq})	Spine-oriented score (h_{spine}^{eff})	Interpretation
ICC (2.1) (inter-rater)	0.84 (95% CI 0.77–0.89)	0.79 (95% CI 0.71–0.86)	"Good" agreement (Koo & Li, 2016)
ICC (2.k) (mean of 5 experts)	0.95	0.92	"Excellent" agreement
Weighted κ	0.78	0.72	"Substantial" (Landis & Koch, 1977)
ICC (2.1) , test–retest	0.90 (95% CI 0.83–0.95)	0.85 (95% CI 0.76–0.92)	High stability
SEM, points	0.80	0.95	Standard error of measurement
MDC_95, points	2.2	2.6	Minimal detectable change

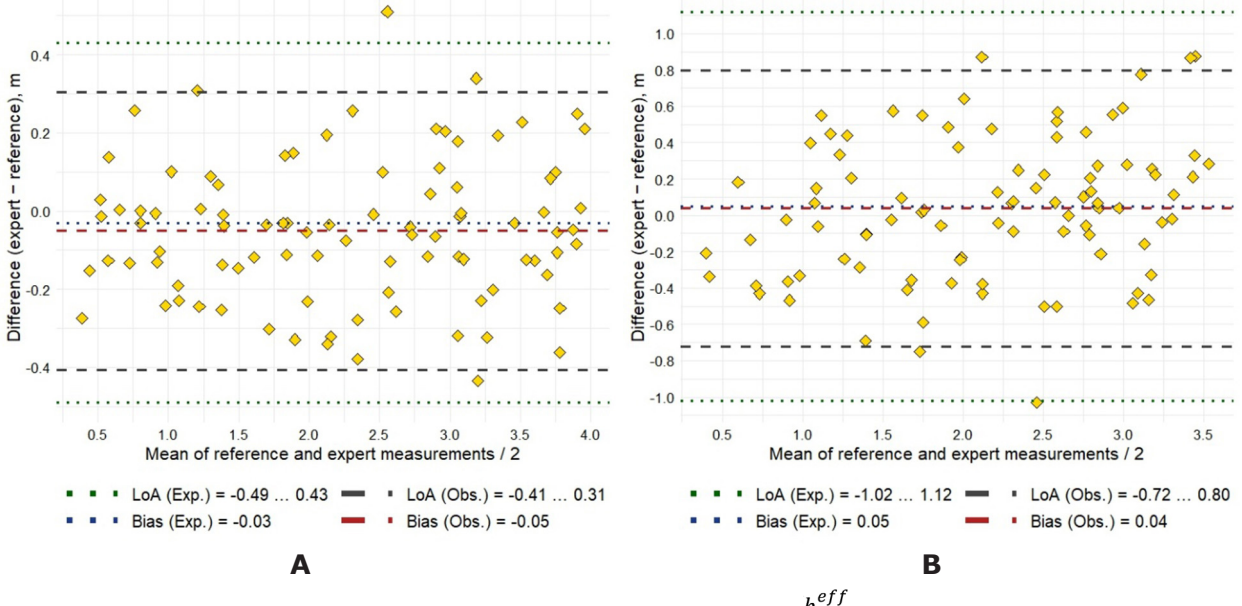

Fig. 4. Bland–Altman plots for the analyzed metrics: A – for heq; B – for h_{spine}^{eff}

For h_{eq} he mean bias was 0,03 m, with 95% limits of agreement (−0.49;0.43) m, for h_{spine}^{eff} − +0.05 m, with 95% limits of agreement (−1.02;1.12) m.

Thus, for the baseline metric h_{eq} near-complete concordance between expert-derived and reference estimates was observed, whereas for h_{spine}^{eff} the limits of agreement were wider. These findings reflect not methodological error but biomechanical uncertainty related to variability in the selection of the deceleration pathway and load-transfer coefficient. Analysis of heteroscedasticity demonstrated that dispersion did not increase at higher or lower metric levels, ensuring comparable precision across the entire range of analyzed values.

Threshold stability. To assess the robustness of score-based classification, a sensitivity analysis was conducted by varying threshold values by ±10–15%, as well as by recalculating scores under "minimal" and "maximal" S_{land} and T_{land} scenarios in the estimation of h_{spine}^{eff}.

For the baseline scale (based on h_{eq}) concordance of the assigned level was maintained in 77% of cases; disagreement by ±1 level occurred in 20%, and by more than ±1 level in only 3%.

For the spine-oriented scale (based on h_{spine}^{eff}) identical level assignment was observed in 62% of cases; a shift of ±1 level occurred in 31%, and of more than ±1 level in 7%.

The greatest sensitivity was noted in transitional scenarios (e.g., falling onto the knees with subsequent axial load transfer) and in landings on soft surfaces, where the potential ranges of S_{land} and T_{land} are broader. Nevertheless, even with parameter variation of 15%, discrepancies in most cases did not exceed one scale level, confirming the practical robustness of the instrument.

Known-groups validity. To evaluate discriminative ability, two clinically relevant groups were compared:

- fragility scenarios: patients ≥65 years old who sustained a fall from a height ≤1 m, typically associated with osteoporotic fractures.

- non-fragility scenarios: younger patients or those injured from falls >1 m and/or in RTAs.

The median h_{spine}^{eff} in the fragility group was 0.48 m (interquartile range 0.32–0.72), whereas in the non-fragility group it was 2.15 m (interquartile range 1.40–3.10). The differences were statistically significant ($p < 0.001$). Cohen's effect size was $d = 1.10$, corresponding to a large effect.

These findings confirm the clinical meaningfulness of the metric: low values of h_{spine}^{eff} are characteristic of low-energy osteoporotic fractures, whereas high values are typical of high-energy trauma requiring different management strategies and associated with a distinct therapeutic prognosis.

Discussion

Interpretation of results and clinical significance

Validation of the multilevel scale for quantitative assessment of external mechanical impact on the spine demonstrated its informativeness and consistency with the actual severity of injury. Higher values of the calculated indices—primarily h_{eq}, h_{spine}^{eff} and $\bar{g}_{spine}$ were statistically associated with more pronounced pathomorphological changes of the spine.

These findings further substantiate the clinical relevance of the metric: low h_{spine}^{eff} values are typical of low-energy osteoporotic fractures, whereas high values correspond to high-energy trauma requiring different therapeutic approaches and associated with different outcome expectations. Elevated h_{eq} and h_{spine}^{eff} were more frequently associated with severe structural damage, and increasing $\bar{g}_{spine}$ reflecting loads exceeding physiologically tolerable limits—was accompanied by a higher probability of severe injury (including categories corresponding to AIS ≥3). This concordance indicates that the scale effectively "captures" the physical "energy of the event" underlying injury severity.

A key advantage of the proposed approach is its quantitative and continuous nature. Instead of descriptive labels, the scale provides numerical values with direct physical interpretation: each increment in h_{eq}, h_{spine}^{eff} and $\bar{g}_{spine}$ corresponds to a real increase in injurious mechanical exposure rather than merely crossing an arbitrary threshold. This enhances clinical interpretability. For example, the conclusion that "the impact is equivalent to a fall from approximately 3 m" can be readily contextualized in terms of expected risk, while load values expressed in units of g are intuitively understood by practicing clinicians.

The results are consistent with clinical experience and epidemiological observations: more intense mechanical exposures (including falls from height and high-speed collisions) are predictably associated with more severe injuries [3, 182], whereas low-energy scenarios (e.g., "standing height or less") more often result in less extensive morphological damage [80, 183]. Importantly, the scale accurately describes the continuum of mechanical exposure: it can be applied to both high- and low-energy events, enabling risk ranking without an a priori assumption regarding the "dominant" mechanism [1, 88].

In practical terms, high values of h_{eq} and h_{spine}^{eff} serve as early indicators of potentially complex spinal injuries (even in the presence of minimal initial symptoms) [153, 184], whereas low values justify a more conservative diagnostic approach [185, 186]. Overall, the scale strengthens the causal link between event biomechanics and clinical outcome, thereby improving the accuracy of risk stratification and supporting evidence-based diagnostic and therapeutic decision-making [187, 188].

Comparison with existing classifications and scales

Abbreviated Injury Scale (AIS) The proposed quantitative approach differs substantially from traditional trauma severity scales. The Abbreviated Injury Scale (AIS) is a widely accepted instrument for grading injury severity based on anatomical damage [17, 18]. AIS assigns injuries scores from 1 (minor) to 6 (maximal, currently untreatable) according to the nature and location of the lesion. However, AIS represents a retrospective assessment—performed after patient evaluation—once specific injuries (fractures, ligament ruptures, spinal cord contusions, etc.) have been identified [153]. AIS neither measures nor describes the mechanism of injury [189]. Moreover, AIS encompasses injuries of the entire body rather than focusing

specifically on the spine; therefore, it inadequately reflects differences in external mechanical exposure. Two patients may receive the same AIS score—for example, AIS 3—although one sustained injury from a fall from height and the other from a high-speed RTA [190].

The scale proposed herein is oriented toward injury biomechanics, i.e., the characteristics of the external impact that caused the damage. It complements AIS by enabling assessment at the stage of mechanism evaluation, prior to definitive diagnosis. For example, knowing that h_{spine}^{eff}> ≈ 5 m allows one to anticipate a high probability of serious spinal injury, even in the absence of obvious signs at initial examination. Thus, the scale functions as a prognostic tool [88]. Similarly, a high h_{eq} value may raise suspicion of injuries to both the musculoskeletal system and internal organs. In contrast, severity according to AIS (e.g., AIS ≥3, typically indicative of serious trauma) is determined only after the injury itself has been documented [191]. Accordingly, the proposed scale does not replace AIS but rather complements the trauma assessment system: AIS ranks severity by consequence, whereas the present scale ranks it by causal factor (impact energy). The integration of both approaches enables a more comprehensive characterization and prognosis of trauma.

Classifications of spinal injuries. Existing classification systems (e.g., AO Spine, TLICS) are primarily oriented toward injury morphology and clinical consequences [19, 192, 193], without providing a quantitative assessment of mechanical exposure [3, 194]. The contemporary international AO Spine Classification System, developed under the auspices of the AO Foundation and partially derived from the Magerl system, categorizes injuries by type (A – compression, B – distraction, C – rotational/ translational injuries), supplemented by neurological status and clinical modifiers, including the condition of the posterior ligamentous complex [195–197]. Its principal strength lies in its comprehensiveness and high reproducibility for guiding management decisions [198]. However, two injuries with the same AO code may result from fundamentally different magnitudes and directions of external load.

The proposed scale quantitatively characterizes the "force of the event" prior to the anatomical outcome, thereby complementing morphological systems. Clinically, this allows the conventional diagnostic formulation (e.g., "AO Spine A3") to be supplemented with the level of mechanical exposure (e.g., "equivalent to a fall from ≈4 m" or the numerical values of h_{eq}, h_{spine}^{eff} and $\bar{g}_{spine}$. Such an approach enhances the prognostic and communicative value of case descriptions: the morphological system specifies what is injured, whereas the quantitative scale indicates the energy/rigidity of the impact that produced the injury [199, 200]. An additional advantage is the mass-neutral and physically interpretable nature of the indicators, which reduces subjectivity and enables valid comparisons across patients and cohorts.

CDC Field Triage Guidelines. In emergency medicine, decisions regarding transport to a trauma center have traditionally relied on mechanism-of-injury criteria [88]. The U.S. National CDC Field Triage Guidelines (developed by the Centers for Disease Control and Prevention in collaboration with the American College of Surgeons) identify several "high-risk mechanisms." For example, an adult fall from >6 m (20 feet) is considered indicative of a high risk of severe trauma and constitutes a criterion for transport to a specialized trauma center [201, 202]. Other "dangerous mechanisms" include significant vehicle deformation (intrusion >30 cm), partial or complete ejection from the vehicle, death of the passenger in the same vehicle, and high-speed motorcycle crashes [5, 199]. The principal advantage of this approach lies in its simplicity and rapid applicability: paramedics can make prompt decisions even when vital signs remain stable [185, 203].

However, the limitations of a threshold-based scheme are evident. Mechanism severity is a continuous variable: the difference between 5.9 m and 6.1 m is negligible, while the threshold itself is conventional [80]. Outcomes are influenced by modifiers that are typically not explicitly incorporated, such as surface type and stiffness, posture/contact geometry, deceleration duration, and the performance of passive safety systems [133, 137, 152]. Consequently, clinical paradoxes arise: a formally "low-energy" event may result in severe injury, whereas a "threshold" event may not [204,205]. This is particularly relevant in vulnerable populations. In older adults, even a fall from standing height may lead to severe cervical injury [82, 183]. Reviews addressing medical triage have also documented substantial rates of under-triage and over-triage, reflecting inevitable information loss when a continuous variable is dichotomized [88].

The proposed quantitative scale complements field triage rules without attempting to replace them. Instead of a binary "threshold exceeded/not exceeded" approach, it provides a graded assessment of mechanical exposure (e.g., h_{eq} 4, 6, or 8 m) and incorporates key modifiers (surface/posture/ S_{land}), such that two falls "from the same height" yield different values when the "rigidity" of contact is fundamentally different. Such integration allows risk differentiation within a given category, potentially reducing both underdiagnosis and unnecessary over-triage. The evolution of medical triage is increasingly oriented toward objective data and telemetry (vehicle parameters/event data recorder, EDR) [171]. In this context, numerical indicators such as (h_{eq}) can be naturally incorporated into EMS algorithms as an additional standardized, evidence-based parameter supporting individualized decision-making [149, 206].

The practical application of the scale lies in its role as a complement—not a substitute—for morphological classifications (e.g., AO Spine, AIS). Quantitative assessment of mechanical exposure is particularly valuable during prehospital triage and patient routing (risk prediction of complex injuries; justification for transport to a trauma center), in planning the scope of imaging, and in multicenter research for standardizing the description of "event severity." In the in-hospital setting, treatment decisions are based primarily on injury morphology and patient status, whereas the scale provides a quantitative context of the mechanism, thereby enhancing communication and risk stratification.

Limitations

This study represents the initial (pilot) stage of scale development and validation. For active implementation in healthcare practice, further calibration of the proposed

indices and expansion of clinical scenarios are required. In particular, external multicenter validation of thresholds and coefficients underlying the calculations is necessary (refinement of T_{land} and S_{land}, the selected reference s_{ref}, and the boundaries of the 0–10 categories). Additional accumulation and analysis of cases with "atypical" mechanics (sliding/oblique contacts, multi-impulse events, compression injuries, blast trauma, multistage falls) are also warranted. Furthermore, the impact of integrating the scale into clinical and organizational decision-making (scope of imaging, patient routing, choice of fixation strategy) on clinical outcomes and resource utilization should be evaluated.

The proposed indicators were optimized for the thoracolumbar junction (T11–L2) as the region most vulnerable to indirect axial loading. Regional adaptation is required for other spinal segments. For example, in the cervical spine, consideration of "head-first" and diving scenarios, as well as whiplash components, is necessary. Overall, this entails the development of segment-specific scenario libraries and recalibration of coefficients accounting for anatomical and biomechanical differences.

Conclusions

The proposed scale represents a mechanistically grounded, mass-neutral, and quantitatively interpretable descriptor of mechanical exposure that complements morphological classifications and is suitable for standardizing trauma description. For clinical implementation, multicenter external validation, refinement of parameters (including calibration of T_{land}, S_{land} and threshold values), and expansion of scenario coverage with consideration of segment-specific biomechanics are required.The technological trajectory involves integration with EMR/EMS systems, utilization of telemetry (EDR, wearable IMU), and automated calculators; the scientific direction includes integration with multibody models and bone quality parameters to develop hybrid risk models.

In light of current clinical and organizational trends (mechanism-oriented triage, harmonization of classifications, and individualization of care), the scale has potential for incorporation into diagnostic and routing protocols, educational modules, and healthcare analytics frameworks. Its implementation may contribute to establishing a unified "language" for quantitative assessment of "event severity," improving data comparability and potentially enhancing the quality of risk stratification and clinical outcomes in spinal trauma.

Acknowledgments

The authors express their gratitude to the experts for their participation in the evaluation of clinical materials, discussion of key methodological decisions, and contributions to the refinement of the proposed scale.

Disclosure

Conflict of interest

The authors declare no conflict of interest.

Informed consent

Informed consent was obtained from each patient.

Funding

The study received no external funding.

References

1. Roberts SB, Tsirikos AI. Biomechanics of the spine and the implications for spinal injuries. Orthopaedics and Trauma. 2024;38(5):258-263. doi: 10.1016/j.mporth.2024.07.001
2. Zileli M, Sharif S, Fornari M. Incidence and Epidemiology of Thoracolumbar Spine Fractures: WFNS Spine Committee Recommendations. Neurospine. 2021;18(4):704-712. doi: 10.14245/ns.2142418.209
3. Iencean SM. Classification of spinal injuries based on the essential traumatic spinal mechanisms. Spinal Cord. 2003;41(7):385-396. doi: 10.1038/sj.sc.3101468
4. Zhaoli M, Hengrui Z, Feiyue L, Hui L, Fei D, Tong L, et al. A Retrospective Epidemiological Study of Patients Hospitalized with Spinal Cord Injury in Dalian Port Hospital from 2017 to 2019. International Journal of Chinese Medicine. 2020;4(4). doi: 10.11648/j.ijcm.20200404.14
5. Kent R, Cormier J, McMurry TL, Johan Ivarsson B, Funk J, Hartka T, Sochor M. Spinal injury rates and specific causation in motor vehicle collisions. Accid Anal Prev. 2023;186:107047. doi: 10.1016/j.aap.2023.107047
6. Neyaz O, Kanaujia V, Yadav RK, Sarkar B, Azam MQ, Kandwal P. Epidemiology of Traumatic Spinal Cord Injury in the Himalayan Range and Sub-Himalayan region: A Retrospective Hospital Data-Based Study. Ann Rehabil Med. 2024;48(1):86-93. doi: 10.5535/arm.23107
7. Wang ZM, Zou P, Yang JS, Liu TT, Song LL, Lu Y, et al. Epidemiological characteristics of spinal cord injury in Northwest China: a single hospital-based study. J Orthop Surg Res. 2020;15(1):214. doi: 10.1186/s13018-020-01729-z
8. Beausejour MH, Wagnac E, Arnoux PJ, Thiong JM, Petit Y. Numerical Investigation of Spinal Cord Injury After Flexion-Distraction Injuries at the Cervical Spine. J Biomech Eng. 2022;144(1). doi: 10.1115/1.4052003
9. Whittier DE, Bevers M, Geusens P, van den Bergh JP, Gabel L. Characterizing Bone Phenotypes Related to Skeletal Fragility Using Advanced Medical Imaging. Curr Osteoporos Rep. 2023;21(6):685-697. doi: 10.1007/s11914-023-00830-6
10. An N, Lin JS, Fei Q. Beijing Friendship Hospital Osteoporosis Self-Assessment Tool for Elderly Male (BFH-OSTM) vs Fracture Risk Assessment Tool (FRAX) for identifying painful new osteoporotic vertebral fractures in older Chinese men: a cross-sectional study. BMC Musculoskelet Disord. 2021;22(1):596. doi: 10.1186/s12891-021-04476-2
11. Ihama F, Pandyan A, Roffe C. Assessment of fracture risk tools in care home residents: a multi-centre observational pilot study. Eur Geriatr Med. 2021;12(1):79-89. doi: 10.1007/s41999-020-00383-2
12. Gibbs JC, MacIntyre NJ, Ponzano M, Templeton JA, Thabane L, Papaioannou A, Giangregorio LM. Exercise for improving outcomes after osteoporotic vertebral fracture. Cochrane Database Syst Rev. 2019;7(7):CD008618. doi: 10.1002/14651858.CD008618.pub3
13. Nau C, Leiblein M, Verboket RD, Horauf JA, Sturm R, Marzi I, Stormann P. Falls from Great Heights: Risk to Sustain Severe Thoracic and Pelvic Injuries Increases with Height of the Fall. J Clin Med. 2021;10(11). doi: 10.3390/jcm10112307
14. Gross C, Menard J, Mull J, Diaz-Zuniga Y, Skarupa D, Crandall M. Assessing Fall Mortality by Field-Relevant Categories at an Urban Level I Trauma Center. J Surg Res. 2024;300:279-286. doi: 10.1016/j.jss.2024.04.008
15. Fujii M, Shirakawa T, Nakamura M, Baba M, Hitosugi M. Factors influencing the injury severity score and the probability of survival in patients who fell from height. Sci Rep. 2021;11(1):15561. doi: 10.1038/s41598-021-95226-w
16. Costachescu B, Popescu CE, Iliescu BF. Analysis of the Classification Systems for Thoracolumbar Fractures in Adults and Their Evolution and Impact on Clinical Management. J Clin Med. 2022;11(9). doi: 10.3390/jcm11092498
17. Gennarelli TA, Wodzin E. AIS 2005: a contemporary injury scale. Injury. 2006;37(12):1083-1091. doi: 10.1016/j.injury.2006.07.009
18. Sahin T, Batin S. A descriptive study of orthopaedic injuries due to parachute jumping in soldiers. BMC Emerg Med. 2020;20(1):58. doi: 10.1186/s12873-020-00354-7

19. Bajamal AH, Permana KR, Faris M, Zileli M, Peev NA. Classification and Radiological Diagnosis of Thoracolumbar Spine Fractures: WFNS Spine Committee Recommendations. Neurospine. 2021;18(4):656-666. doi: 10.14245/ns.2142650.325
20. Hwang Z, Abdalla M, Ajayi B, Bernard J, Bishop T, Lui DF. Thoracolumbar spine trauma: a guide for the FRCS examination. Eur J Orthop Surg Traumatol. 2023;33(6):2655-2661. doi: 10.1007/s00590-022-03430-9
21. Vu C, Gendelberg D. Classifications in Brief: AO Thoracolumbar Classification System. Clin Orthop Relat Res. 2020;478(2):434-440. doi: 10.1097/CORR.0000000000001086
22. Jeanmougin T, Cole E, Duceau B, Raux M, James A. Heterogeneity in defining multiple trauma: a systematic review of randomized controlled trials. Crit Care. 2023;27(1):363. doi: 10.1186/s13054-023-04637-w
23. Donnelly NA, Brent L, Hickey P, Masterson S, Deasy C, Moloney J, et al. Substantial heterogeneity in trauma triage tool characteristic operationalization for identification of major trauma: a hybrid systematic review. Eur J Trauma Emerg Surg. 2025;51(1):74. doi: 10.1007/s00068-024-02694-6
24. Wohlgemut JM, Marsden MER, Stoner RS, Pisirir E, Kyrimi E, Grier G, et al. Diagnostic accuracy of clinical examination to identify life- and limb-threatening injuries in trauma patients. Scand J Trauma Resusc Emerg Med. 2023;31(1):18. doi: 10.1186/s13049-023-01083-z
25. Xiong T, Luo Q, Chen Q, Shi L, Duan A, Liu S, Li K. Development of a repetitive traumatic brain injury risk function based on real-world accident reconstruction and wavelet packet energy analysis. Front Bioeng Biotechnol. 2025;13:1548265. doi: 10.3389/fbioe.2025.1548265
26. Mokkink LB, Prinsen CA, Bouter LM, Vet HC, Terwee CB. The COnsensus-based Standards for the selection of health Measurement INstruments (COSMIN) and how to select an outcome measurement instrument. Braz J Phys Ther. 2016;20(2):105-113. doi: 10.1590/bjpt-rbf.2014.0143
27. Swan K, Speyer R, Scharitzer M, Farneti D, Brown T, Woisard V, Cordier R. Measuring what matters in healthcare: a practical guide to psychometric principles and instrument development. Front Psychol. 2023;14:1225850. doi: 10.3389/fpsyg.2023.1225850
28. Mokkink LB, de Vet H, Diemeer S, Eekhout I. Sample size recommendations for studies on reliability and measurement error: an online application based on simulation studies. Health Services and Outcomes Research Methodology. 2022;23(3):241-265. doi: 10.1007/s10742-022-00293-9
29. Lewis CC, Klasnja P, Lyon AR, Powell BJ, Lengnick-Hall R, Buchanan G, et al. The mechanics of implementation strategies and measures: advancing the study of implementation mechanisms. Implement Sci Commun. 2022;3(1):114. doi: 10.1186/s43058-022-00358-3
30. Galhardas L, Raimundo A, Marmeleira J. Test-retest reliability of upper-limb proprioception and balance tests in older nursing home residents. Arch Gerontol Geriatr. 2020;89:104079. doi: 10.1016/j.archger.2020.104079
31. Hage R, Detrembleur C, Dierick F, Brismee JM, Roussel N, Pitance L. Sensorimotor performance in acute-subacute non-specific neck pain: a non-randomized prospective clinical trial with intervention. BMC Musculoskelet Disord. 2021;22(1):1017. doi: 10.1186/s12891-021-04876-4
32. Gatsonis C, Sampson AR. Multiple correlation: exact power and sample size calculations. Psychol Bull. 1989;106(3):516-524. doi: 10.1037/0033-2909.106.3.516
33. Hattie J, Cooksey RW. Procedures for Assessing the Validities of Tests Using the "Known-Groups" Method. Applied Psychological Measurement. 1984;8(3):295-305. doi: 10.1177/014662168400800306
34. Kalcev G, Barbov I, Kotevska PI, Preti A, Carta MG. Biological Rhythms in People from North Macedonia with Bipolar Disorder: Application of the Macedonian Biological Rhythms Interview of Assessment in Neuropsychiatry (BRIAN). The Open Psychology Journal. 2022;15(1). doi: 10.2174/18743501-v15-e2208301
35. Hiraishi M, Tanioka K, Shimokawa T. Concordance rate of a four-quadrant plot for repeated measurements. BMC Med Res Methodol. 2021;21(1):270. doi: 10.1186/s12874-021-01461-0
36. Jan SL, Shieh G. The Bland-Altman range of agreement: Exact interval procedure and sample size determination. Comput Biol Med. 2018;100:247-252. doi: 10.1016/j.compbiomed.2018.06.020
37. Taffe P, Zuppinger C, Burger GM, Nussle SG. The Bland-Altman method should not be used when one of the two measurement methods has negligible measurement errors. PLoS One. 2022;17(12):e0278915. doi: 10.1371/journal.pone.0278915
38. Bansal A, Heagerty PJ. A comparison of landmark methods and time-dependent ROC methods to evaluate the time-varying performance of prognostic markers for survival outcomes. Diagn Progn Res. 2019;3:14. doi: 10.1186/s41512-019-0057-6
39. Seshan VE, Gonen M, Begg CB. Comparing ROC curves derived from regression models. Stat Med. 2013;32(9):1483-1493. doi: 10.1002/sim.5648
40. Ruxton GD, Wilkinson DM, Neuhäuser M. Advice on testing the null hypothesis that a sample is drawn from a normal distribution. Animal Behaviour. 2015;107:249-252. doi: 10.1016/j.anbehav.2015.07.006
41. Shapiro SS, Wilk MB. An analysis of variance test for normality (complete samples). Biometrika. 1965;52(3-4):591-611. doi: 10.1093/biomet/52.3-4.591
42. Bahariniya S, Ezatiasar M, Madadizadeh F. A Brief Review of the Types of Validity and Reliability of scales in Medical Research. Journal of Community Health Research. 2021. doi: 10.18502/jchr.v10i2.6582
43. de Winter JC, Gosling SD, Potter J. Comparing the Pearson and Spearman correlation coefficients across distributions and sample sizes: A tutorial using simulations and empirical data. Psychol Methods. 2016;21(3):273-290. doi: 10.1037/met0000079
44. Schober P, Vetter TR. Logistic Regression in Medical Research. Anesth Analg. 2021;132(2):365-366. doi: 10.1213/ANE.0000000000005247
45. Zabor EC, Reddy CA, Tendulkar RD, Patil S. Logistic Regression in Clinical Studies. Int J Radiat Oncol Biol Phys. 2022;112(2):271-277. doi: 10.1016/j.ijrobp.2021.08.007
46. Abreu MN, Siqueira AL, Cardoso CS, Caiaffa WT. Ordinal logistic regression models: application in quality of life studies. Cad Saude Publica. 2008;24 Suppl 4:s581-591. doi: 10.1590/s0102-311x2008001600010
47. Guzman-Castillo M, Brailsford S, Luke M, Smith H. A tutorial on selecting and interpreting predictive models for ordinal health-related outcomes. Health Services and Outcomes Research Methodology. 2015;15(3-4):223-240. doi: 10.1007/s10742-015-0140-6
48. Zeng G. A graphic and tabular variable deduction method in logistic regression. Communications in Statistics - Theory and Methods. 2020;51(16):5412-5427. doi: 10.1080/03610926.2020.1839499
49. Discacciati A, Palazzolo MG, Park JG, Melloni GEM, Murphy SA, Bellavia A. Estimating and presenting non-linear associations with restricted cubic splines. Int J Epidemiol. 2025;54(4). doi: 10.1093/ije/dyaf088
50. Schuster NA, Rijnhart JJM, Twisk JWR, Heymans MW. Modeling non-linear relationships in epidemiological data: The application and interpretation of spline models. Front Epidemiol. 2022;2:975380. doi: 10.3389/fepid.2022.975380
51. Shrestha N. Detecting Multicollinearity in Regression Analysis. American Journal of Applied Mathematics and Statistics. 2020;8(2):39-42. doi: 10.12691/ajams-8-2-1
52. Corbacioglu SK, Aksel G. Receiver operating characteristic curve analysis in diagnostic accuracy studies: A guide to interpreting the area under the curve value. Turk J Emerg Med. 2023;23(4):195-198. doi: 10.4103/tjem.tjem_182_23
53. Ruopp MD, Perkins NJ, Whitcomb BW, Schisterman EF. Youden Index and optimal cut-point estimated from observations affected by a lower limit of detection. Biom J. 2008;50(3):419-430. doi: 10.1002/bimj.200710415
54. Paiva JRB, Pacheco VMG, Barbosa PS, Almeida FR, Wainer GA, Gomes FA, et al. Complexity measure based on sensitivity analysis applied to an intensive care unit system. Scientific Reports. 2023;13(1):14602. doi: 10.1038/s41598-023-40149-x

55. den Boon S, Jit M, Brisson M, Medley G, Beutels P, White R, et al. Guidelines for multi-model comparisons of the impact of infectious disease interventions. BMC Medicine. 2019;17(1):163. doi: 10.1186/s12916-019-1403-9
56. Kien C, Schultes MT, Szelag M, Schoberberger R, Gartlehner G. German language questionnaires for assessing implementation constructs and outcomes of psychosocial and health-related interventions: a systematic review. Implement Sci. 2018;13(1):150. doi: 10.1186/s13012-018-0837-3
57. Williams ZJ, Failla MD, Davis SL, Heflin BH, Okitondo CD, Moore DJ, Cascio CJ. Thermal Perceptual Thresholds are typical in Autism Spectrum Disorder but Strongly Related to Intra-individual Response Variability. Sci Rep. 2019;9(1):12595. doi: 10.1038/s41598-019-49103-2
58. Vargha A, Delaney HD. A Critique and Improvement of the CL Common Language Effect Size Statistics of McGraw and Wong. Journal of Educational and Behavioral Statistics. 2000;25(2):101-132. doi: 10.3102/10769986025002101
59. Panjeh S, Nordahl-Hansen A, Cogo-Moreira H. Establishing new cutoffs for Cohen's d: An application using known effect sizes from trials for improving sleep quality on composite mental health. Int J Methods Psychiatr Res. 2023;32(3):e1969. doi: 10.1002/mpr.1969. PMID: 37186318
60. Bobak CA, Barr PJ, O'Malley AJ. Estimation of an inter-rater intra-class correlation coefficient that overcomes common assumption violations in the assessment of health measurement scales. BMC Med Res Methodol. 2018;18(1):93. doi: 10.1186/s12874-018-0550-6
61. Kvalseth TO. An Alternative Interpretation of the Linearly Weighted Kappa Coefficients for Ordinal Data. Psychometrika. 2018. doi: 10.1007/s11336-018-9621-1
62. Mitani AA, Freer PE, Nelson KP. Summary measures of agreement and association between many raters' ordinal classifications. Ann Epidemiol. 2017;27(10):677-685 e674. doi: 10.1016/j.annepidem.2017.09.001
63. Polit DF. Getting serious about test-retest reliability: a critique of retest research and some recommendations. Qual Life Res. 2014;23(6):1713-1720. doi: 10.1007/s11136-014-0632-9
64. Bland JM, Altman DG. Measuring agreement in method comparison studies. Stat Methods Med Res. 1999;8(2):135-160. doi: 10.1177/096228029900800204
65. Chan PY, Mohd Ripin Z, Abdul Halim S, Kamarudin MI, Ng KS, Eow GB, et al. Biomechanical System Versus Observational Rating Scale for Parkinson's Disease Tremor Assessment. Sci Rep. 2019;9(1):8117. doi: 10.1038/s41598-019-44142-1
66. Stratford PW, Riddle DL. When minimal detectable change exceeds a diagnostic test-based threshold change value for an outcome measure: resolving the conflict. Phys Ther. 2012;92(10):1338-1347. doi: 10.2522/ptj.20120002
67. Bonovas S, Piovani D. On p-Values and Statistical Significance. J Clin Med. 2023;12(3). doi: 10.3390/jcm12030900
68. Sharma H. Statistical significance or clinical significance? A researcher's dilemma for appropriate interpretation of research results. Saudi J Anaesth. 2021;15(4):431-434. doi: 10.4103/sja.sja_158_21
69. Gonzalvez M, Munoz-Hernandez C. R programming environment in wildlife: Are Veterinary Sciences at the same level than other research areas? Res Vet Sci. 2024;166:105079. doi: 10.1016/j.rvsc.2023.105079
70. Ivancevic VG. New Mechanics of Spinal Injury. International Journal of Applied Mechanics. 2012;01(02):387-401. doi: 10.1142/s1758825109000174
71. LaPlaca MC, Simon CM, Prado GR, Cullen DK. CNS injury biomechanics and experimental models. Prog Brain Res. 2007;161:13-26. doi: 10.1016/S0079-6123(06)61002-9
72. Teresinski G, Milaszkiewicz A, Cywka T. An analysis of the relationship between bodily injury severity and fall height in victims of fatal falls from height. Arch Med Sadowej Kryminol. 2016;66(3):133-140. doi: 10.5114/amsik.2016.66397
73. Casali MB, Blandino A, Grignaschi S, Florio EM, Travaini G, Genovese UR. The pathological diagnosis of the height of fatal falls: A mathematical approach. Forensic Sci Int. 2019;302:109883. doi: 10.1016/j.forsciint.2019.109883
74. Petrone N, Cognolato M, McNeil JA, Hubbard M. Designing, building, measuring, and testing a constant equivalent fall height terrain park jump. Sports Engineering. 2017;20(4):283-292. doi: 10.1007/s12283-017-0253-y
75. Liu C, Xu T, Xia W, Xu S, Zhu Z, Zhou M, Liu H. Incidence, prevalence, and causes of spinal injuries in China, 1990-2019: Findings from the Global Burden of Disease Study 2019. Chin Med J (Engl). 2024;137(6):704-710. doi: 10.1097/CM9.0000000000003045
76. Lu Y, Shang Z, Zhang W, Pang M, Hu X, Dai Y, et al. Global incidence and characteristics of spinal cord injury since 2000-2021: a systematic review and meta-analysis. BMC Med. 2024;22(1):285. doi: 10.1186/s12916-024-03514-9
77. Gnanaprakash G, Peddireddy S, Kanna RM, Shetty AP, Rajasekaran S. Spinal Injuries Due to Falls from Height. Indian Spine Journal. 2024;7(2):168-174. doi: 10.4103/isj.isj_75_23
78. Goodacre S, Than M, Goyder EC, Joseph AP. Can the distance fallen predict serious injury after a fall from a height? J Trauma. 1999;46(6):1055-1058. doi: 10.1097/00005373-199906000-00014
79. Palacio C, Darwish M, Acosta M, Bautista R, Hovorka M, Chen C, Hovorka J. Incidence of fall-from-height injuries and predictive factors for severity. J Osteopath Med. 2025;125(5):229-236. doi: 10.1515/jom-2024-0158
80. Zhang ZR, Wu Y, Wang FY, Wang WJ. Traumatic spinal cord injury caused by low falls and high falls: a comparative study. J Orthop Surg Res. 2021;16(1):222. doi: 10.1186/s13018-021-02379-5
81. Koch M, Lunde LK, Gjulem T, Knardahl S, Veiersted KB. Validity of Questionnaire and Representativeness of Objective Methods for Measurements of Mechanical Exposures in Construction and Health Care Work. PLoS One. 2016;11(9):e0162881. doi: 10.1371/journal.pone.0162881
82. Bruggink C, van de Ree CLP, van Ditshuizen J, Polinder-Bos HA, Oner FC, Reijman M, Rutges J. Increased incidence of traumatic spinal injury in patients aged 65 years and older in the Netherlands. Eur Spine J. 2024;33(10):3677-3684. doi: 10.1007/s00586-024-08310-w
83. Wang F, Sun R, Zhang SD, Wu XT. Comparison of thoracolumbar versus non-thoracolumbar osteoporotic vertebral compression fractures in risk factors, vertebral compression degree and pre-hospital back pain. J Orthop Surg Res. 2023;18(1):643. doi: 10.1186/s13018-023-04140-6
84. Bodmer NS, Hauselmann HJ, Frey D, Aeberli D, Bachmann LM. Expert consensus on relevant risk predictors for the occurrence of osteoporotic fractures in specific clinical subgroups - Delphi survey. BMC Rheumatol. 2019;3:50. doi: 10.1186/s41927-019-0099-y
85. Kanis JA, McCloskey EV, Harvey NC, Cooper C, Rizzoli R, Dawson-Hughes B, et al. Intervention thresholds and diagnostic thresholds in the management of osteoporosis. Aging Clin Exp Res. 2022;34(12):3155-3157. doi: 10.1007/s40520-022-02216-7
86. Wool NK, Wilson S, Chong ACM, Dart BR. Bone Health Improvement Protocol. Kansas Journal of Medicine. 2017;10(3):62-66. doi: 10.17161/kjm.v10i3.8659
87. McCoy CE, Chakravarthy B, Lotfipour S. Guidelines for Field Triage of Injured Patients: In conjunction with the Morbidity and Mortality Weekly Report published by the Center for Disease Control and Prevention. West J Emerg Med. 2013;14(1):69-76. doi: 10.5811/westjem.2013.1.15981
88. Haske D, Lefering R, Stock JP, Kreinest M, TraumaRegister DGU. Epidemiology and predictors of traumatic spine injury in severely injured patients: implications for emergency procedures. Eur J Trauma Emerg Surg. 2022;48(3):1975-1983. doi: 10.1007/s00068-020-01515-w
89. Braken P, Amsler F, Gross T. Simple modification of trauma mechanism alarm criteria published for the TraumaNetwork DGU((R)) may significantly improve overtriage - a cross sectional study. Scand J Trauma Resusc Emerg Med. 2018;26(1):32. doi: 10.1186/s13049-018-0498-x
90. Basiratzadeh S, Hakimjavadi R, Baddour N, Michalowski W, Viktor H, Wai E, et al. A data-driven approach to categorize patients with traumatic spinal cord injury: cluster analysis of a multicentre database. Front Neurol. 2023;14:1263291.

doi: 10.3389/fneur.2023.1263291
91. Yokogawa N, Kato S, Sasagawa T, Hayashi H, Tsuchiya H, Ando K, et al. Differences in clinical characteristics of cervical spine injuries in older adults by external causes: a multicenter study of 1512 cases. Sci Rep. 2022;12(1):15867. doi: 10.1038/s41598-022-19789-y
92. Wu Y, Zhang Z, Wang F, Wang W. Current status of traumatic spinal cord injury caused by traffic accident in Northern China. Sci Rep. 2022;12(1):13892. doi: 10.1038/s41598-022-16930-9
93. Yuan H, Guo Q, Zhang Z, Ou L, Wang H, Yu H, Xiang L. Sex, age, role and geographic differences in traumatic spinal fractures caused by motor vehicle collisions: a multicentre retrospective study. Sci Rep. 2023;13(1):3712. doi: 10.1038/s41598-023-30982-5
94. Breitlauch P, Erbsmehl CT, van Ratingen M, Mallada JL, Sandner V, Ferson N, Urban M. A novel method for the automated simulation of various vehicle collisions to estimate crash severity. Traffic Inj Prev. 2023;24(sup1):S116-S123. doi: 10.1080/15389588.2022.2159761
95. Pinter K, Szalay Z, Vida G. Road Accident Reconstruction Using On-board Data, Especially Focusing on the Applicability in Case of Autonomous Vehicles. Periodica Polytechnica Transportation Engineering. 2020;49(2):139-145. doi: 10.3311/PPtr.13469
96. Vida G, Török Á. Effects of developing data recording technologies on the reliability of accident reconstruction and liability determination. European Transport Research Review. 2025;17(1). doi: 10.1186/s12544-025-00727-8
97. Bastien C, Wellings R, Burnett B. An evidence based method to calculate pedestrian crossing speeds in vehicle collisions (PCSC). Accid Anal Prev. 2018;118:66-76. doi: 10.1016/j.aap.2018.05.020
98. Ogura A. Analyzing collisions in classical mechanics using mass–momentum diagrams. European Journal of Physics. 2017;38(5):055001. doi: 10.1088/1361-6404/aa750b
99. Chatterjee A, James G, Brogliato B. Approximate coefficient of restitution for nonlinear viscoelastic contact with external load. Granular Matter. 2022;24(4). doi: 10.1007/s10035-022-01284-w
100. Meyer N, Wagemann EL, Jackstadt A, Seifried R. Material and particle size sensitivity analysis on coefficient of restitution in low-velocity normal impacts. Computational Particle Mechanics. 2022;9(6):1293-1308. doi: 10.1007/s40571-022-00471-z
101. Seifried R, Schiehlen W, Eberhard P. Numerical and experimental evaluation of the coefficient of restitution for repeated impacts. International Journal of Impact Engineering. 2005;32(1-4):508-524. doi: 10.1016/j.ijimpeng.2005.01.001
102. Green I. The prediction of the coefficient of restitution between impacting spheres and finite thickness plates undergoing elastoplastic deformations and wave propagation. Nonlinear Dynamics. 2022;109(4):2443-2458. doi: 10.1007/s11071-022-07522-3
103. Higham JE, Shepley P, Shahnam M. Measuring the coefficient of restitution for all six degrees of freedom. Granular Matter. 2019;21(2). doi: 10.1007/s10035-019-0871-0
104. Hunt KH, Crossley FRE. Coefficient of Restitution Interpreted as Damping in Vibroimpact. Journal of Applied Mechanics. 1975;42(2):440-445. doi: 10.1115/1.3423596
105. Reyes A, Børvik T. Quasi-static behaviour of crash components with steel skins and polymer foam cores. Materials Today Communications. 2018;17:541-553. doi: 10.1016/j.mtcomm.2018.09.015
106. Wang D, Zhang J, Wang S, Hu L. Frontal Vehicular Crash Energy Management Using Analytical Model in Multiple Conditions. Sustainability. 2022;14(24). doi: 10.3390/su142416913
107. Gidlewski M, Prochowski L, Jemioł L, Żardecki D. The process of front-to-side collision of motor vehicles in terms of energy balance. Nonlinear Dynamics. 2018;97(3):1877-1893. doi: 10.1007/s11071-018-4688-x
108. Brach RM, Brach RM, Pongetti K. Analysis of High-Speed Sideswipe Collisions Using Data from Small Overlap Tests. SAE International Journal of Transportation Safety. 2014;02(1):86-99. doi: 10.4271/2014-01-0469
109. Davison TM, Collins GS. Complex Crater Formation by Oblique Impacts on the Earth and Moon. Geophysical Research Letters. 2022;49(21). doi: 10.1029/2022gl101117
110. Li S, Anis M, Lord D, Zhang H, Zhou Y, Ye X. Beyond 1D and oversimplified kinematics: A generic analytical framework for surrogate safety measures. Accid Anal Prev. 2024;204:107649. doi: 10.1016/j.aap.2024.107649
111. Statler TS, Raducan SD, Barnouin OS, DeCoster ME, Chesley SR, Barbee B, et al. After DART: Using the First Full-scale Test of a Kinetic Impactor to Inform a Future Planetary Defense Mission. The Planetary Science Journal. 2022;3(10). doi: 10.3847/PSJ/ac94c1
112. Stickle AM, DeCoster ME, Burger C, Caldwell WK, Graninger D, Kumamoto KM, et al. Effects of Impact and Target Parameters on the Results of a Kinetic Impactor: Predictions for the Double Asteroid Redirection Test (DART) Mission. The Planetary Science Journal. 2022;3(11). doi: 10.3847/PSJ/ac91cc
113. Ataei M, Khajepour A, Jeon S. A general rollover index for tripped and un-tripped rollovers on flat and sloped roads. Proceedings of the Institution of Mechanical Engineers, Part D: Journal of Automobile Engineering. 2017;233(2):304-316. doi: 10.1177/0954407017743345
114. Viano DC, Parenteau CS, Edwards ML. Rollover injury: effects of near- and far-seating position, belt use, and number of quarter rolls. Traffic Inj Prev. 2007;8(4):382-392. doi: 10.1080/15389580701583379
115. Dobbertin KM, Freeman MD, Lambert WE, Lasarev MR, Kohles SS. The relationship between vehicle roof crush and head, neck and spine injury in rollover crashes. Accid Anal Prev. 2013;58:46-52. doi: 10.1016/j.aap.2013.04.020
116. Freeman MD, Dobbertin K, Kohles SS, Uhrenholt L, Eriksson A. Serious head and neck injury as a predictor of occupant position in fatal rollover crashes. Forensic Sci Int. 2012;222(1-3):228-233. doi: 10.1016/j.forsciint.2012.06.003
117. Heller MF, Newberry WN, Smedley JE, Eswaran SK, Croteau JJ, Carhart MR. Occupant Kinematics and Injury Mechanisms During Rollover in a High Strength-to-Weight Ratio Vehicle. SAE International Journal of Passenger Cars - Mechanical Systems. 2010;03(1):450-466. doi: 10.4271/2010-01-0516
118. Kazemian AH, Fooladi M, Darijani H. Rollover Index for the Diagnosis of Tripped and Untripped Rollovers. Latin American Journal of Solids and Structures. 2017;14(11):1979-1999. doi: 10.1590/1679-78253576
119. Ikhsan N, Saifizul A, Ramli R. The Effect of Vehicle and Road Conditions on Rollover of Commercial Heavy Vehicles during Cornering: A Simulation Approach. Sustainability. 2021;13(11). doi: 10.3390/su13116337
120. El-Rich M, Arnoux PJ, Wagnac E, Brunet C, Aubin CE. Finite element investigation of the loading rate effect on the spinal load-sharing changes under impact conditions. J Biomech. 2009;42(9):1252-1262. doi: 10.1016/j.jbiomech.2009.03.036
121. Davidson PL, Wilson SJ, Wilson BD, Chalmers DJ. An approach to modeling impact energy absorption by surfaces. J Appl Biomech. 2009;25(4):351-359. doi: 10.1123/jab.25.4.351
122. Shimizu T, Yoshitani K. Impact-reduction effect of tatami floor mat made of nonwoven fabric for head injuries in fall accidents. Journal of Building Engineering. 2019;24. doi: 10.1016/j.jobe.2019.02.020
123. Wei W, Evin M, Bailly N, Arnoux PJ. Biomechanical evaluation of Back injuries during typical snowboarding backward falls. Scand J Med Sci Sports. 2023;33(3):224-234. doi: 10.1111/sms.14254
124. Mattucci S, Speidel J, Liu J, Kwon BK, Tetzlaff W, Oxland TR. Basic biomechanics of spinal cord injury - How injuries happen in people and how animal models have informed our understanding. Clin Biomech (Bristol). 2019;64:58-68. doi: 10.1016/j.clinbiomech.2018.03.020
125. Rao RD, Delbar K, Yoganandan N. Body Morphology and Its Associations With Thoracolumbar Trauma Sustained in Motor Vehicle Collisions. J Am Acad Orthop Surg. 2015;23(12):769-777. doi: 10.5435/JAAOS-D-15-00277
126. Yoganandan N, Moore J, DeVogel N, Pintar F, Banerjee A, Baisden J, et al. Human lumbar spinal column injury

criteria from vertical loading at the base: Applications to military environments. J Mech Behav Biomed Mater. 2020;105:103690. doi: 10.1016/j.jmbbm.2020.103690
127. Bose D, Crandall JR, Untaroiu CD, Maslen EH. Influence of pre-collision occupant parameters on injury outcome in a frontal collision. Accid Anal Prev. 2010;42(4):1398-1407. doi: 10.1016/j.aap.2010.03.004
128. Kimpara H, Lee JB, Yang KH, King AI. Effects of body weight, height, and rib cage area moment of inertia on blunt chest impact response. Traffic Inj Prev. 2010;11(2):207-214. doi: 10.1080/15389580903554863
129. Khorasani-Zavareh D, Bigdeli M, Saadat S, Mohammadi R. Kinetic energy management in road traffic injury prevention: a call for action. J Inj Violence Res. 2015;7(1):36-37. doi: 10.5249/jivr.v7i1.458
130. Palanca M, Perilli E, Martelli S. Body Anthropometry and Bone Strength Conjointly Determine the Risk of Hip Fracture in a Sideways Fall. Ann Biomed Eng. 2021;49(5):1380-1390. doi: 10.1007/s10439-020-02682-y
131. Rostro-González H, Puigoriol-Forcada JM, Pérez-Peña A, Menacho J, Garcia-Granada A-A. Optimizing crash box design to meet injury criteria: a protocol for accurate simulation and material selection. Structural and Multidisciplinary Optimization. 2024;67(8). doi: 10.1007/s00158-024-03855-2
132. Bahlsen A, Nigg BM. Influence of Attached Masses on Impact Forces and Running Style in Heel-Toe Running. International Journal of Sport Biomechanics. 1987;3(3):264-275. doi: 10.1123/ijsb.3.3.264
133. Bhan S, Levine IC, Laing AC. Energy absorption during impact on the proximal femur is affected by body mass index and flooring surface. J Biomech. 2014;47(10):2391-2397. doi: 10.1016/j.jbiomech.2014.04.026
134. Somasundaram K, Humm JR, Yoganandan N, Hauschild H, Driesslein K, Pintar FA. Obese Occupant Response in Reclined and Upright Seated Postures in Frontal Impacts. Stapp Car Crash J. 2022;66:31-68. doi: 10.4271/2022-22-0002
135. Raj N, Krishnapillai S. An improved spinal injury parameter model for underbody impulsive loading scenarios. Int J Numer Method Biomed Eng. 2020;36(3):e3307. doi: 10.1002/cnm.3307
136. Ferenczi MA, Bershitsky SY, Koubassova NA, Kopylova GV, Fernandez M, Narayanan T, Tsaturyan AK. Why muscle is an efficient shock absorber. PLoS One. 2014;9(1):e85739. doi: 10.1371/journal.pone.0085739
137. Cutlan R, Khokhar M, Shammout N, Shah AS, Frazer L, Yoganandan N, et al. Lumbar Spine Orientation Affects Compressive Fracture Outcome. Ann Biomed Eng. 2024. doi: 10.1007/s10439-024-03604-y
138. Yoganandan N, Moore J, Pintar FA, Banerjee A, DeVogel N, Zhang J. Role of disc area and trabecular bone density on lumbar spinal column fracture risk curves under vertical impact. J Biomech. 2018;72:90-98. doi: 10.1016/j.jbiomech.2018.02.030
139. Schwarze M, Hurschler C, Welke B. Force, impulse and energy during falling with and without knee protection: an in-vitro study. Sci Rep. 2019;9(1):10336. doi: 10.1038/s41598-019-46880-8
140. Tamura A, Akasaka K, Otsudo T. Energy Absorption Strategies in the Lower Extremities during Double-Leg Landings in Knee Valgus Alignment. Applied Sciences. 2020;10(23). doi: 10.3390/app10238742
141. Ivancic PC. Biomechanics of Thoracolumbar Burst and Chance-Type Fractures during Fall from Height. Global Spine J. 2014;4(3):161-168. doi: 10.1055/s-0034-1381729
142. Amiri S, Naserkhaki S, Parnianpour M. Assessment of lumbar spinal disc injury in frontal crashes. Comput Biol Med. 2020;123:103846. doi: 10.1016/j.compbiomed.2020.103846
143. Pachocki L, Daszkiewicz K, Luczkiewicz P, Witkowski W. Biomechanics of Lumbar Spine Injury in Road Barrier Collision-Finite Element Study. Front Bioeng Biotechnol. 2021;9:760498. doi: 10.3389/fbioe.2021.760498
144. Ivancic PC. Cervical spine instability following axial compression injury: a biomechanical study. Orthop Traumatol Surg Res. 2014;100(1):127-133. doi: 10.1016/j.otsr.2013.10.015
145. Hajiaghamemar M, Seidi M, Ferguson JR, Caccese V. Measurement of Head Impact Due to Standing Fall in Adults Using Anthropomorphic Test Dummies. Ann Biomed Eng. 2015;43(9):2143-2152. doi: 10.1007/s10439-015-1255-1
146. Ivancic PC. Instabilité du rachis cervical par traumatisme en compression axiale : une étude biomécanique. Revue de Chirurgie Orthopédique et Traumatologique. 2014;100(1). doi: 10.1016/j.rcot.2013.10.091
147. Li L, Baur M, Baldwin K, Kuehn T, Zhu Q, Herman D, Dai B. Falling as a strategy to decrease knee loading during landings: Implications for ACL injury prevention. J Biomech. 2020;109:109906. doi: 10.1016/j.jbiomech.2020.109906
148. Li M, Zhang D, Liu Q, Zhang T. Driver Injury from Vehicle Side Impacts When Automatic Emergency Braking and Active Seat Belts Are Used. Sensors (Basel). 2023;23(13). doi: 10.3390/s23135821
149. Mishra E, Mroz K, Pipkorn B, Lubbe N. Effects of Automated Emergency Braking and Seatbelt Pre-Pretensioning on Occupant Injury Risks in High-Severity Frontal Crashes. Frontiers in Future Transportation. 2022;3. doi: 10.3389/ffutr.2022.883951
150. Tamura A, Akasaka K, Otsudo T. Contribution of Lower Extremity Joints on Energy Absorption during Soft Landing. Int J Environ Res Public Health. 2021;18(10). doi: 10.3390/ijerph18105130
151. Van Toen C, Melnyk AD, Street J, Oxland TR, Cripton PA. The effect of lateral eccentricity on failure loads, kinematics, and canal occlusions of the cervical spine in axial loading. J Biomech. 2014;47(5):1164-1172. doi: 10.1016/j.jbiomech.2013.12.001
152. Van Toen C, Sran MM, Robinovitch SN, Cripton PA. Transmission of force in the lumbosacral spine during backward falls. Spine (Phila Pa 1976). 2012;37(9):E519-527. doi: 10.1097/BRS.0b013e31823ecae0
153. Whyte T, Melnyk AD, Van Toen C, Yamamoto S, Street J, Oxland TR, Cripton PA. A neck compression injury criterion incorporating lateral eccentricity. Sci Rep. 2020;10(1):7114. doi: 10.1038/s41598-020-63974-w
154. Yeow CH, Lee PV, Goh JC. Effect of landing height on frontal plane kinematics, kinetics and energy dissipation at lower extremity joints. J Biomech. 2009;42(12):1967-1973. doi: 10.1016/j.jbiomech.2009.05.017
155. Giatsis G, Panoutsakopoulos V, Kollias IA. Drop Jumping on Sand Is Characterized by Lower Power, Higher Rate of Force Development and Larger Knee Joint Range of Motion. J Funct Morphol Kinesiol. 2022;7(1). doi: 10.3390/jfmk7010017
156. Harris DA, Spears IR. The effect of rugby shoulder padding on peak impact force attenuation. Br J Sports Med. 2010;44(3):200-203. doi: 10.1136/bjsm.2008.047449
157. Jung S. Water entry and exit in nature: review. Interface Focus. 2025;15(2):20240055. doi: 10.1098/rsfs.2024.0055
158. Kerdok AE, Biewener AA, McMahon TA, Weyand PG, Herr HM. Energetics and mechanics of human running on surfaces of different stiffnesses. J Appl Physiol (1985). 2002;92(2):469-478. doi: 10.1152/japplphysiol.01164.2000
159. Lachance CC, Jurkowski MP, Dymarz AC, Robinovitch SN, Feldman F, Laing AC, Mackey DC. Compliant flooring to prevent fall-related injuries in older adults: A scoping review of biomechanical efficacy, clinical effectiveness, cost-effectiveness, and workplace safety. PLoS One. 2017;12(2):e0171652. doi: 10.1371/journal.pone.0171652
160. Laforest S, Robitaille Y, Dorval D, Lesage D, Pless B. Severity of fall injuries on sand or grass in playgrounds. J Epidemiol Community Health. 2000;54(6):475-477. doi: 10.1136/jech.54.6.475
161. Laing AC, Robinovitch SN. Low stiffness floors can attenuate fall-related femoral impact forces by up to 50% without substantially impairing balance in older women. Accid Anal Prev. 2009;41(3):642-650. doi: 10.1016/j.aap.2009.03.001
162. Laing AC, Tootoonchi I, Hulme PA, Robinovitch SN. Effect of compliant flooring on impact force during falls on the hip. J Orthop Res. 2006;24(7):1405-1411. doi: 10.1002/jor.20172
163. Mackey DC, Lachance CC, Wang PT, Feldman F, Laing AC, Leung PM, et al. The Flooring for Injury Prevention (FLIP) Study of compliant flooring for the prevention of fall-related injuries in long-term care: A randomized trial. PLoS Med. 2019;16(6):e1002843. doi: 10.1371/journal.pmed.1002843

164. Nakanishi T, Hitosugi M, Murayama H, Takeda A, Motozawa Y, Ogino M, Koyama K. Biomechanical Analysis of Serious Neck Injuries Resulting from Judo. Healthcare (Basel). 2021;9(2). doi: 10.3390/healthcare9020214
165. Qu H, Zhang S, Sorochan JC, Weinhandl JT, Thoms AW, Dickson KH. Effects of synthetic turf and shock pad on impact attenuation related biomechanics during drop landing. Sports Biomech. 2022;21(6):748-760. doi: 10.1080/14763141.2019.1690570
166. Tessutti V, Ribeiro AP, Trombini-Souza F, Sacco IC. Attenuation of foot pressure during running on four different surfaces: asphalt, concrete, rubber, and natural grass. J Sports Sci. 2012;30(14):1545-1550. doi: 10.1080/02640414.2012.713975
167. Tomin M, Kossa A, Berezvai S, Kmetty Á. Investigating the impact behavior of wrestling mats via finite element simulation and falling weight impact tests. Polymer Testing. 2022;108. doi: 10.1016/j.polymertesting.2022.107521
168. Wardiningsih W, Troynikov O. An evaluation of force attenuation, comfort properties and density of materials for hip protective pads. Journal of Engineered Fibers and Fabrics. 2019;14. doi: 10.1177/1558925019853955
169. Schafer R, Trompeter K, Fett D, Heinrich K, Funken J, Willwacher S, et al. The mechanical loading of the spine in physical activities. Eur Spine J. 2023;32(9):2991-3001. doi: 10.1007/s00586-023-07733-1
170. Huang Q, Kleiven S. Finite Element Analysis of Energy-Absorbing Floors for Reducing Head Injury Risk during Fall Accidents. Applied Sciences. 2023;13(24). doi: 10.3390/app132413260
171. Mishra E, Lubbe N. Assessing injury risks of reclined occupants in a frontal crash preceded by braking with varied seatbelt designs using the SAFER Human Body Model. Traffic Inj Prev. 2024;25(3):445-453. doi: 10.1080/15389588.2024.2318414
172. Harper DJ, McBurnie AJ, Santos TD, Eriksrud O, Evans M, Cohen DD, et al. Biomechanical and Neuromuscular Performance Requirements of Horizontal Deceleration: A Review with Implications for Random Intermittent Multi-Directional Sports. Sports Med. 2022;52(10):2321-2354. doi: 10.1007/s40279-022-01693-0
173. Stemper BD, Chirvi S, Doan N, Baisden JL, Maiman DJ, Curry WH, et al. Biomechanical tolerance of whole lumbar spines in straightened posture subjected to axial acceleration. J Orthop Res. 2018;36(6):1747-1756. doi: 10.1002/jor.23826
174. Chastain K, Gepner B, Moreau D, Koerber B, Forman J, Hallman J, Kerrigan J. Effect of axial compression on stiffness and deformation of human lumbar spine in flexion-extension. Traffic Inj Prev. 2023;24(sup1):S55-S61. doi: 10.1080/15389588.2023.2198627
175. Gabauer DJ, Gabler HC. The effects of airbags and seatbelts on occupant injury in longitudinal barrier crashes. J Safety Res. 2010;41(1):9-15. doi: 10.1016/j.jsr.2009.10.006
176. Soica A, Gheorghe C. A Review of Seatbelt Technologies and Their Role in Vehicle Safety. Applied Sciences. 2025;15(10). doi: 10.3390/app15105303
177. Pintar FA, Yoganandan N, Myers T, Elhagediab A, Sances A, Jr. Biomechanical properties of human lumbar spine ligaments. J Biomech. 1992;25(11):1351-1356. doi: 10.1016/0021-9290(92)90290-h
178. Sequeira GJ, Brandmeier T. Evaluation and characterization of crash-pulses for head-on collisions with varying overlap crash scenarios. Transportation Research Procedia. 2020;48:1306-1315. doi: 10.1016/j.trpro.2020.08.156
179. King AI, Yang KH. Research in biomechanics of occupant protection. J Trauma. 1995;38(4):570-576. doi: 10.1097/00005373-199504000-00017
180. Hans D, Goertzen AL, Krieg MA, Leslie WD. Bone microarchitecture assessed by TBS predicts osteoporotic fractures independent of bone density: the Manitoba study. J Bone Miner Res. 2011;26(11):2762-2769. doi: 10.1002/jbmr.499
181. Schreiber JJ, Anderson PA, Rosas HG, Buchholz AL, Au AG. Hounsfield units for assessing bone mineral density and strength: a tool for osteoporosis management. J Bone Joint Surg Am. 2011;93(11):1057-1063. doi: 10.2106/jbjs.J.00160
182. Wang TY, Park C, Zhang H, Rahimpour S, Murphy KR, Goodwin CR, et al. Management of Acute Traumatic Spinal Cord Injury: A Review of the Literature. Front Surg. 2021;8:698736. doi: 10.3389/fsurg.2021.698736
183. Grabel ZJ, Lunati MP, Segal DN, Kukowski NR, Yoon ST, Jain A. Thoracolumbar spinal fractures associated with ground level falls in the elderly: An analysis of 254,486 emergency department visits. J Clin Orthop Trauma. 2020;11(5):916-920. doi: 10.1016/j.jcot.2020.04.009
184. Chen S, Li G, Li F, Wang G, Wang Q. A dynamic nomogram for predicting the probability of irreversible neurological dysfunction after cervical spinal cord injury: research based on clinical features and MRI data. BMC Musculoskelet Disord. 2023;24(1):459. doi: 10.1186/s12891-023-06570-z
185. Kreinest M, Gliwitzky B, Schuler S, Grutzner PA, Munzberg M. Development of a new Emergency Medicine Spinal Immobilization Protocol for trauma patients and a test of applicability by German emergency care providers. Scand J Trauma Resusc Emerg Med. 2016;24:71. doi: 10.1186/s13049-016-0267-7
186. Maschmann C, Jeppesen E, Rubin MA, Barfod C. New clinical guidelines on the spinal stabilisation of adult trauma patients - consensus and evidence based. Scand J Trauma Resusc Emerg Med. 2019;27(1):77. doi: 10.1186/s13049-019-0655-x
187. Mohammad Ismail A, Forssten MP, Hildebrand F, Sarani B, Ioannidis I, Cao Y, et al. Cardiac risk stratification and adverse outcomes in surgically managed patients with isolated traumatic spine injuries. Eur J Trauma Emerg Surg. 2024;50(2):523-530. doi: 10.1007/s00068-023-02413-7
188. Dao QA, Nguyen VS, Dang VQ, Tran PC, Le DTS. Diagnostic accuracy and clinical utility of mTLICS versus TLICS and TL AOSIS in stratifying three-tier treatment for thoracolumbar injuries: focus on intermediate score range. BMC Musculoskelet Disord. 2025;26(1):824. doi: 10.1186/s12891-025-09124-7/
189. Loftis KL, Price J, Gillich PJ. Evolution of the Abbreviated Injury Scale: 1990-2015. Traffic Inj Prev. 2018;19(sup2):S109-S113. doi: 10.1080/15389588.2018.1512747
190. van Wessem KJP, Niemeyer MJS, Leenen LPH. Polytrauma patients with severe cervical spine injuries are different than with severe TBI despite similar AIS scores. Sci Rep. 2022;12(1):21538. doi: 10.1038/s41598-022-25809-8
191. Germanetti F, Fiumarella D, Belingardi G, Scattina A. Injury Criteria for Vehicle Safety Assessment: A Review with a Focus Using Human Body Models. Vehicles. 2022;4(4):1080-1095. doi: 10.3390/vehicles4040057
192. Lee JY, Vaccaro AR, Lim MR, Oner FC, Hulbert RJ, Hedlund R, et al. Thoracolumbar injury classification and severity score: a new paradigm for the treatment of thoracolumbar spine trauma. J Orthop Sci. 2005;10(6):671-675. doi: 10.1007/s00776-005-0956-y
193. Patel AA, Vaccaro AR. Thoracolumbar spine trauma classification. J Am Acad Orthop Surg. 2010;18(2):63-71. doi: 10.5435/00124635-201002000-00001
194. Fradet L, Petit Y, Wagnac E, Aubin CE, Arnoux PJ. Biomechanics of thoracolumbar junction vertebral fractures from various kinematic conditions. Med Biol Eng Comput. 2014;52(1):87-94. doi: 10.1007/s11517-013-1124-8
195. Karamian BA, Schroeder GD, Lambrechts MJ, Canseco JA, Oner C, Vialle E, et al. An international validation of the AO spine subaxial injury classification system. Eur Spine J. 2023;32(1):46-54. doi: 10.1007/s00586-022-07467-6
196. Schnake KJ, Schroeder GD, Vaccaro AR, Oner C. AOSpine Classification Systems (Subaxial, Thoracolumbar). J Orthop Trauma. 2017;31 Suppl 4:S14-S23. doi: 10.1097/BOT.0000000000000947
197. Vaccaro AR, Oner C, Kepler CK, Dvorak M, Schnake K, Bellabarba C, et al. AOSpine thoracolumbar spine injury classification system: fracture description, neurological status, and key modifiers. Spine (Phila Pa 1976). 2013;38(23):2028-2037. doi: 10.1097/BRS.0b013e3182a8a381
198. Schroeder GD, Karamian BA, Canseco JA, Vialle LR, Kandziora F, Benneker LM, et al. Validation of the AO Spine Sacral Classification System: Reliability Among Surgeons Worldwide. J Orthop Trauma. 2021;35(12):e496-e501. doi: 10.1097/BOT.0000000000002110

199. Bak AB, Moghaddamjou A, Malvea A, Fehlings MG. Impact of Mechanism of Injury on Long-term Neurological Outcomes of Cervical Sensorimotor Complete Acute Traumatic Spinal Cord Injury. Neurospine. 2022;19(4):1049-1056. doi: 10.14245/ns.2244518.259
200. Goulet J, Richard-Denis A, Petit Y, Diotalevi L, Mac-Thiong JM. Morphological features of thoracolumbar burst fractures associated with neurological outcome in thoracolumbar traumatic spinal cord injury. Eur Spine J. 2020;29(10):2505-2512. doi: 10.1007/s00586-020-06420-9
201. Newgard CD, Fischer PE, Gestring M, Michaels HN, Jurkovich GJ, Lerner EB, Fallat ME, Delbridge TR, Brown JB, Bulger EM; Writing Group for the 2021 National Expert Panel on Field Triage. National guideline for the field triage of injured patients: Recommendations of the National Expert Panel on Field Triage, 2021. J Trauma Acute Care Surg. 2022 Aug 1;93(2):e49-e60. doi: 10.1097/TA.0000000000003627
202. Lokerman RD, van Rein EAJ, Waalwijk JF, van der Sluijs R, Houwert RM, Lansink KWW, et al. Accuracy of Prehospital Triage of Adult Patients With Traumatic Injuries Following Implementation of a Trauma Triage Intervention. JAMA Network Open. 2023;6(4):e236805-e236805. doi: 10.1001/jamanetworkopen.2023.6805
203. Geduld C, Muller H, Saunders CJ. Factors which affect the application and implementation of a spinal motion restriction protocol by prehospital providers in a low resource setting: A scoping review. Afr J Emerg Med. 2022;12(4):393-405. doi: 10.1016/j.afjem.2022.08.005
204. caravantes R, Quezada A, Jimenez L. Low-energy trauma causing multiple cervical fracture: a case report. MOJ Surgery. 2024;12(3):117-119. doi: 10.15406/mojs.2024.12.00276
205. Freeman MD, Croft AC, Nicodemus CN, Centeno CJ, Elkins WL. Significant spinal injury resulting from low-level accelerations: a case series of roller coaster injuries. Arch Phys Med Rehabil. 2005;86(11):2126-2130. doi: 10.1016/j.apmr.2005.05.017
206. Yoganandan N, Stemper BD, Baisden JL, Pintar FA, Paskoff GR, Shender BS. Effects of acceleration level on lumbar spine injuries in military populations. Spine J. 2015;15(6):1318-1324. doi: 10.1016/j.spinee.2013.07.486